DRUG DISCOVERY TARGETING THE INTERACTION OF MLL-AF4 WITH AF9 IN PEDIATRIC MLL-REARRANGED LEUKEMIA

by

Yu Peng

A thesis submitted to the Faculty of the University of Delaware in partial fulfillment of the requirements for the degree of Master of Science in Biological Sciences

Fall 2013

DRUG DISCOVERY TARGETING THE INTERACTION OF MLL-AF4 WITH AF9 IN PEDIATRIC MLL-REARRANGED LEUKEMIA

by

Yu Peng

Approved: _____
Salil A. Lachke, Ph.D.
Professor in charge of thesis on behalf of the Advisory Committee

Approved: _____
Andrew D. Napper, Ph.D.
Professor in charge of thesis on behalf of the Advisory Committee

Approved: _____
Randall L. Duncan, Ph.D.
Chair of the Department of Biological Sciences

Approved: _____
George H. Watson, Ph.D.
Dean of the College of Arts and Sciences

Approved: _____
James G. Richards, Ph.D.
Vice Provost for Graduate and Professional Education

ACKNOWLEDGMENTS

First and foremost, I'd like to thank my advisor, Dr. Andrew Napper. I would never have been able to finish my thesis without your patient guidance. I am so grateful for the time I have spent under your tutelage. Thank you very much for taking me as you graduate student when I was not sure whether I could continue my study in Delaware. I benefited a lot from the discussion with you, especially your positive attitude at work will affect my whole life. Also, thank you for supporting and understanding my choice for pursuing another degree.

I would like to thank Dr. Zhihao Zhuang from Department of Chemistry and Biochemistry. Thank you for giving me the chance to work in your lab three years ago and reminding to develop good lab habits, which helped me a lot in my later work. Thank you for trusting me and giving me my own project, even I did not have much Biochemical background. If it was not you, I would never had chance to meet my phenomenal advisor.

I am very grateful to my committee members, Dr. Anja Nohe and Dr. Salil Lachke who has through their guidance and support that has shaped my project to where it is today.

I would like to thank my lab members: Venita Watson, Donna Cartledge, and Asmita Kumar, who have always offered helping hands. Thank you, also, Kathy, thanks for guiding me and sharing your wealth of knowledge with me in the past three years. Thank you for teaching me how to use various software and passing this wonderful project to me.

I would like to thank all the SNERPs and my fellow “first years”, particularly Priyanka Dhanan, I would never forget the days we fought side-by-side to prepare the prelim and study together. Also, I would like to thank my best friend Di Wu, thank you for being such a great buddy.

Most importantly, I would like to thank my families, without their support I would never made this far. Also, thank you my loving wife, Qin Liang, who always there cheering me up and stood by me through the good time and bad.

TABLE OF CONTENTS

LIST OF TABLES

LIST OF FIGURES

ABSTRACT

Rearrangement of the mixed-lineage leukemia (MLL) in pediatric leukemia is generally a predictor of a very poor prognosis. These chromosomal rearrangements result in fusion of the protein MLL to one of more than 60 protein partners. MLL fusions are potent inducers of leukemia through activation of oncogene expression; therefore, targeting this transcriptional activation function may arrest MLL-rearranged (MLL-R) leukemia. Leukemic cell lines harboring the most common fusion protein, MLL-AF4, require the direct interaction of AF4 with the transcription factor AF9 to survive and self-renew. Disrupting this interaction with a cell-penetrating AF4-derived peptide results in cell death, suggesting that the AF4-AF9 interaction could be a viable target for a novel MLL-R leukemia therapy. To discover chemical compounds that disrupt AF4-AF9 binding, I used a high-throughput screening (HTS) assay using homogeneous proximity-based AlphaScreen technology to detect non-peptidic inhibitors of AF4-AF9 binding. The assay had been previously validated in the HTS lab by screening small compound libraries containing 5,680 compounds. I confirmed the activity of hits from this pilot screen by testing in dose response, and further characterized the most promising active compound. After pilot screening, I used this assay to screen a library from the Lankenau Chemical Genomics Center (LCGC) comprising 96,000 orthogonally pooled compounds. The assay was also transferred to the Broad Institute (Cambridge, MA) and used to screen 350,000 compounds from the NIH collection. I confirmed hits from both screens by testing in dose-response, and identified one hit

from the Broad Institute screening with promising activity. All other remaining hits from both the Broad Institute and LCGC screening were found to be artifacts interfering with the assay. In an attempt to improve potency of the two promising hits from the Nemours pilot screen and the Broad Institute HTS, analogs were synthesized in Dr. John Koh's lab at the University of Delaware (Department of Chemistry and Biochemistry) and tested by me at Nemours. Work will continue to further optimize inhibitors of the interaction of MLL-AF4 and AF9 so that these may be tested in leukemia cells and ultimately as potential therapeutics for MLL-R leukemia.

Chapter 1

INTRODUCTION

1.1 MLL- Rearranged Leukemia

MLL-R leukemia is an aggressive pediatric cancer that arises from translocations involving the *MLL* (mixed lineage leukemia) gene, so called because the resulting disease displays characteristics of both acute lymphocytic leukemia (ALL) and acute myelogenous leukemia (AML). ALL and AML together account for approximately one third of childhood cancers. Translocations of the *MLL* gene leads to MLL fusion proteins, which are the most important characteristic of MLL-R leukemia [1]. These MLL rearrangements are especially prevalent in infant ALL, occurring in 80% of cases, and also in 75% of therapy-related AML. The 5-year survival rate for ALL without MLL rearrangement approaches 90%; in stark contrast, infants with ALL harboring MLL rearrangements only have a 40% survival rate [2, 3]. Thus specifically targeted therapies are urgently needed.

MLL is an ortholog of the Drosophila gene Trithorax, whose products play important roles in embryogenesis, in part by binding the promoters of *HOX* genes and maintaining the expression of these genes [4-7]. MLL protein is a large multidomain protein commonly expressed in hematopoietic cells. In normal cells, MLL, a histone methyltransferase, is responsible for methylating the lysine 4 residue on histone 3 (H3K4) and regulating the expression of genes that have an essential role in the development of the hematopoietic system, leading to normal differentiation of the

hematopoietic cells (Fig. 1.1 A). In leukemic cells, chromosomal rearrangements lead to loss of the C-terminal methyltransferase domain of MLL, giving rise to oncogenic fusion proteins comprising the N-terminus of MLL linked to one of more than 60 partner proteins. However, 5 fusion partners account for 80% of cases of MLL-R leukemia, and of these the MLL-AF4 fusion is the most prevalent. The MLL-AF4 has been shown to bind to AF9, which in turn recruits cyclin T and protein kinase CDK9, and the histone methytransferase DOT1L, which promote transcription by phosphorylation of RNA polymerase II and methylation of lysine 79 in histone 3, respectively (Fig 1.1 B). Therefore, these MLL fusions are potent inducers of leukemia; through mechanisms that are still unclear, the fusion proteins cause abnormal expression of specific *MLL* target genes, notably the homeobox (*HOX*) genes [8-10], which are normally tightly regulated to ensure normal hematopoiesis. Overexpression of the oncogene *HOXA9* in particular is repeatedly found in MLL-R leukemia. A loss of control of gene expression at a critical stage in hematopoietic development blocks differentiation of hematopoietic cell progenitors, which acquire the capacity for unlimited self-renewal, leading to malignant transformation [2, 10].

A

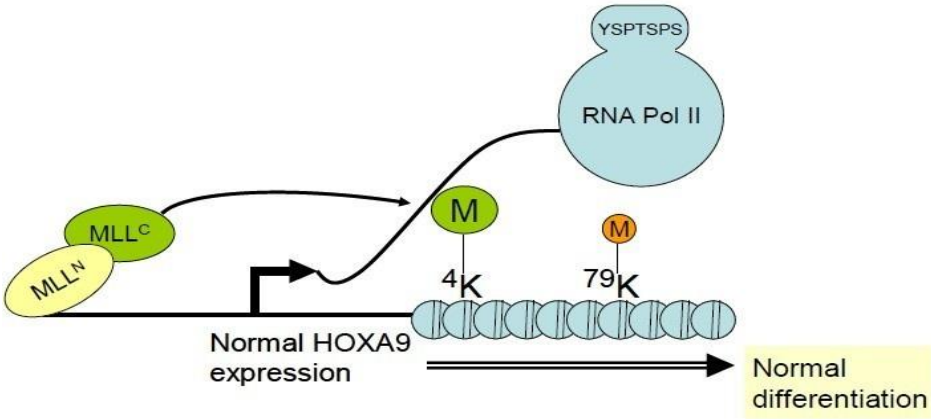

B

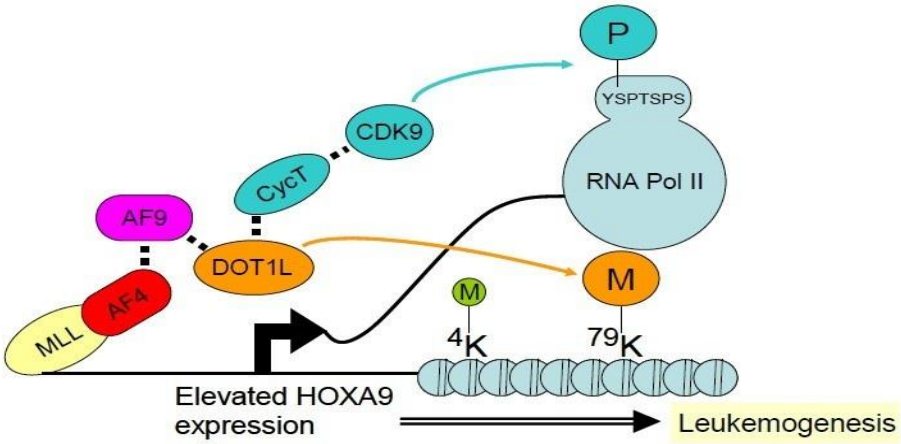

Fig. 1.1 Transcriptional targets. (A) Normal function of MLL, leading to normal differentiation of hematopoietic cells. (B) Rearrangement of MLL, leading to leukemogenesis.

1.2 Hypothesis and Drug Discovery Approach to MLL-R Leukemia

Recent studies have found that MLL fusions affect gene expression by recruiting a complex of proteins, including several transcription factors and the histone methyltransferase DOT1L, which regulate the activity of RNA polymerase II during transcriptional elongation (Fig. 1.1 B) [2, 11, 12]. Therefore, we hypothesized that disruption of one or more of the key protein–protein interactions within the transcriptional elongation complex may block MLL-R leukemia and restore normal hematopoietic differentiation. Among these MLL fusions, MLL-AF4 is the most common fusion; in infants, it is associated with the worst prognosis, and alone accounts for half of the leukemia cases [13, 14]. Therefore, for this project we decided to focus our initial efforts on MLL-AF4 due to its importance in high-risk pediatric leukemia and based on published work that revealed MLL-AF4 and AF9 could be a potential target against MLL-R leukemia [15, 16].

Hemenway and coworkers mapped the AF9 binding domain of AF4 and found that the direct interaction between AF4 and the transcription factor AF9 is required for proliferation and survival of leukemic cell lines harboring the MLL-AF4 fusion [16, 17]. Yeast two-hybrid assays identified a 12-amino-acid sequence in AF4 that binds to the C-terminus of AF9, and a 10-amino acid peptide sequence derived from the 12-mer was the smallest peptide found to have activity in vitro. Both of the two peptides potently inhibited binding of AF9 to AF4 with a single-digit nanomolar half-maximal inhibition concentration (IC_{50}) potency in an enzyme linked immune sorbent assay (ELISA). Moreover, a cell-permeable penetratin-containing peptide called PFWT (penetratin-LWVKIDLDLLSRV) was shown by fluorescence microscopy to disrupt intracellular AF4-AF9 binding. This cell-penetrating peptide caused leukemia cell

lines harboring the MLL-AF4 fusion to undergo cell death. However, it did not affect the viability of hematopoietic progenitor cells [15, 16].

Further studies demonstrated synergy between the AF9-binding peptide and conventional chemotherapeutic agents in the selective killing of leukemia cells containing MLL-AF4 [15, 18]. The peptide work of Hemenway and coworkers demonstrates that targeting the AF4-AF9 interaction could be a viable therapeutic strategy against leukemia harboring MLL-AF4 fusions and provides proof of principle for our small-molecule drug discovery efforts. The relatively small size of the peptide that inhibits the AF4-AF9 binding interaction suggests that it should be possible to identify small non-peptidic AF9 antagonists [19].

1.3 HTS Strategy

This study aimed to screen for inhibitors of the interaction between the transcription factors AF4 and AF9 using a high-throughput assay. To this end, a homogeneous AlphaScreen assay was developed and optimized in the Nemours HTS lab by Kathy Drake and Venita Watson [20] to measure the binding between a biotinylated peptide derived from the AF9-binding site of AF4 and FLAG-tagged AF9 protein (full-length). In this Thesis I describe screening of compound libraries comprising 201,608 compounds in the Nemours Center for Childhood Cancer Research (A.I. DuPont hospital for Children, Wilmington, DE). Compounds were screened in 384-well plates either as a single compound per well or orthogonally pooled (10 compounds/well). The assay was also transferred to the Broad Institute (Cambridge, MA) to screen 350,000 compounds from the NIH collection. Hits were confirmed by dose-response testing, and work is ongoing to optimize the most promising active compounds by chemical synthesis and testing of analogs in

collaboration with Dr. John Koh's lab at the University of Delaware (Department of Chemistry and Biochemistry).

Chapter 2

MATERIALS & METHODS

2.1 Materials

2.1.1 Reagents and Materials

Potassium phosphate monobasic, potassium phosphate dibasic, sodium chloride (NaCl), DMSO, isopropanol and Tween-20 were obtained from Fisher Chemicals (Waltham, MA). Phosphate-buffered saline (PBS, pH 7.4) was made up to a final concentration of 1.47 mM potassium phosphate monobasic, 4.3 mM sodium phosphate dibasic, 2.7 mM potassium chloride, and 137 mM NaCl. Fluorescein sodium salt and Nunc 384-well black & clear plates were from Sigma-Aldrich (St. Louis, MO). 384-well white AlphaScreen SW, 7.5% bovine serum albumin (BSA), P30 MDT tips (Catalog no. 13180252) and AlphaScreen FLAG detection kit (Catalog no. 6760613C) containing anti-FLAG-coated acceptor beads and streptavidin donor beads were purchased from Perkin Elmer. VP 540-100 Lint-free blotting media were purchased from V&P Scientific (San Diego, CA). Biotin-FLAG peptide used in the counterscreen (sequence: Biotin-GGSGGSGGSGGSGGSGGDYKDDDDK); N-terminal biotinylated AF4 27-mer (residues 748–773), representing the AF9-binding region of AF4; and non-biotinylated peptides (Table 2.1) were from Biomatik (Wilmington, DE). We chose to use these peptides to replicate the results found by Srinivasan et al. [16]. The AF9 protein possessing a C-terminal FLAG tag was

custom-expressed and purified by Origene (Rockville, MD). Corning 3095 microplate sealing tape was obtained from Fisher Scientific (Morris Plains, NJ).

Table 2.1. AF4 peptide sequences

Peptide	**Sequence** [a]
Biotin-AF4 27-mer [b]	Biotin-LSPLRDTPPPQS**LMVKITLDLL**SRIPQ-OH
AF4 27-mer	NH2-LSPLRDTPPPQS**LMVKITLDLL**SRIPQ-OH
8-mer [c]	NH2-**WVKIDLDL**-OH
10-mer	NH2-**LWVKIDLDLL**-OH
12-mer	NH2-**LWVKIDLDLL**SR-OH
12-mer (inactive) [d]	NH2-**LWEKSDLDLL**SR-OH

[a] Residues key to AF9 binding are in bold type.

[b] The biotinylated and non-biotinylated AF4 27-mer peptides are derived from residues 747-774 of AF4.

[c] The 8, 10, and 12-mer peptides are derived from the homologue FMR2 which is closely related to AF4 and shares the AF9 interaction domain.

[d] Underline indicates substituted amino acids.

2.1.2 Compound Libraries

The Spectrum Collection compound library comprising 2,000 U.S. Food and Drug Administration–approved drugs and bioactive natural products at 10 mM concentration in DMSO was obtained from MicroSource, Inc. (Gaylordsville, CT) [21]. The library was reformatted into polypropylene V-bottom 384-well microplates obtained from Greiner BioOne (Catalog no. 781280; Monroe, NC) at 4 mM in 10 μL DMSO. The first and last two columns were filled with 10 μL DMSO.

The Natural Products Library (NPL) and Natural Derivatives Library (NDL) were obtained from TimTec (Newark, DE) [22]. The NPL contained 680 natural products, and the NDL contained 3,000 synthetic compounds whose design is based on natural product–derived scaffolds. The compounds from these libraries at 10 mM in 100 μL DMSO were reformatted from 96- to 384-well plates and diluted to 2 mM

with 10 μL DMSO in polypropylene round-bottom plates from Nalge Nunc International (Catalog no. 264573; Rochester, NY). The first and last two columns were filled with 10 μL DMSO.

The ChemBridge library (Chembridge, San Diego, CA) comprises 100,000 compounds at 10 mM in 100 μL DMSO in Corning Costar clear V-bottom 96-well plates, and were reformatted into 313 orthogonally pooled Nunc 384-well clear plates. The first and last columns were filled with 100 μL DMSO.

The MicroSource, TimTec and Chembridge libraries were non-pooled libraries, consisting of one compound in each well. In contrast, the LCGC library (Lankenau Institute for Medical Research, Wynnewood, PA) comprises 96,000 compounds mixed 10-per-well at a total concentration of 5 mM or 10 mM in 5 μL DMSO in Nunc 384-well black round-bottom plates.

2.2 Methods

2.2.1 High-Throughput Screening

2.2.1.1 Liquid Transfers

Liquid transfers were performed on a JANUS MDT. All transfer speeds with P30 tips were set at 4 µL/sec with 1 µL blowout and 2 seconds delay. Aspiration and dispense height were set at 0.4 mm and 0.3 mm above well bottom, respectively. For pintool transfer, pins dipped 6 times into well bottom in source plate and target plate with 2 seconds delay, and speed of liquid entry and retraction were set at 10 mm/sec.

2.2.1.2 HTS Wash Procedure

All the wash procedures were as described in *Table 2.2 A* and *Table 2.2 B.* For step 2 of the pintool transfer, the wash solution was made of 110 mL 1:1 water and DMSO mixture. This was due to pintool transferred compounds in DMSO. Same reason for step 2 of tip wash that contained 500 mL 1:1 water and DMSO mixture. For both tips and pintool, the dispense height were 1 mm deeper than the aspiration height. And also each aspiration height was 1 mm deeper than the previous dispense height. An extra wash step with an isopropanol wash/flush station was added exclusively for pintool, since the regular wash was not able to efficiently clean the slots in the pins.

Table 2.2. A. Tip wash procedure

Tip wash step	Parameter	ASP volume (µL)	ASP height below liquid surface (mm)	DSP volume (µL)	DSP height below liquid surface (mm)	Pause (sec)	Repeat
1	1st blot	0	0	0	0	5	0
2	500 mL 1:1 water & DMSO mixture or 500 mL water	20	4	20	5	0	5
3	2nd blot	0	0	0	0	5	0
4	500 mL ispropanol	25	6	25	7	0	5
5	3rd blot	0	0	0	0	5	0
6	Air dry	30	/	30	/	/	15

Table 2.2. B. Pintool wash procedure

Pintool wash step	Parameter	ASP volume (µL)	ASP height below liquid surface (mm)	DSP volume (µL)	DSP height below liquid surface (mm)	Pause (sec)	Repeat
1	1st blot	/	0	/	0	5	0
2	110 mL 1:1 waster & DMSO mixture	/	4	/	5	0	5
3	2nd blot	/	0	/	0	5	0
4	500 mL ispropanol	/	6	/	7	0	5
5	Isopropanol wash/flush station	/	8	/	9	0	5
6	3rd blot	/	0	/	0	5	0
7	Air dry	/	/	/	/	180	/

ASP, aspiration; DSP, dispense.

2.2.1.3 Homogeneous AlphaScreen Assay

A high-throughput assay to screen for inhibitors of the interaction between the transcription factors AF4 and AF9 was established using AlphaScreen technology. Binding of a biotinylated AF4 peptide to FLAG-tagged AF9 protein is detected by the addition of streptavidin-coated donor beads and anti-FLAG-coated acceptor beads. If peptide and protein are bound, laser excitation of the donor beads results in singlet oxygen ($^1O_2$) transfer to the acceptor beads and light emission (Fig. 2.1 A). A small-molecule inhibitor disrupts the peptide–protein binding, causing singlet oxygen transfer fails to occur due to the increased distance between the donor and acceptor beads. Thus, inhibitor binding is detectable by a decrease in light emission (Fig. 2.1 B).

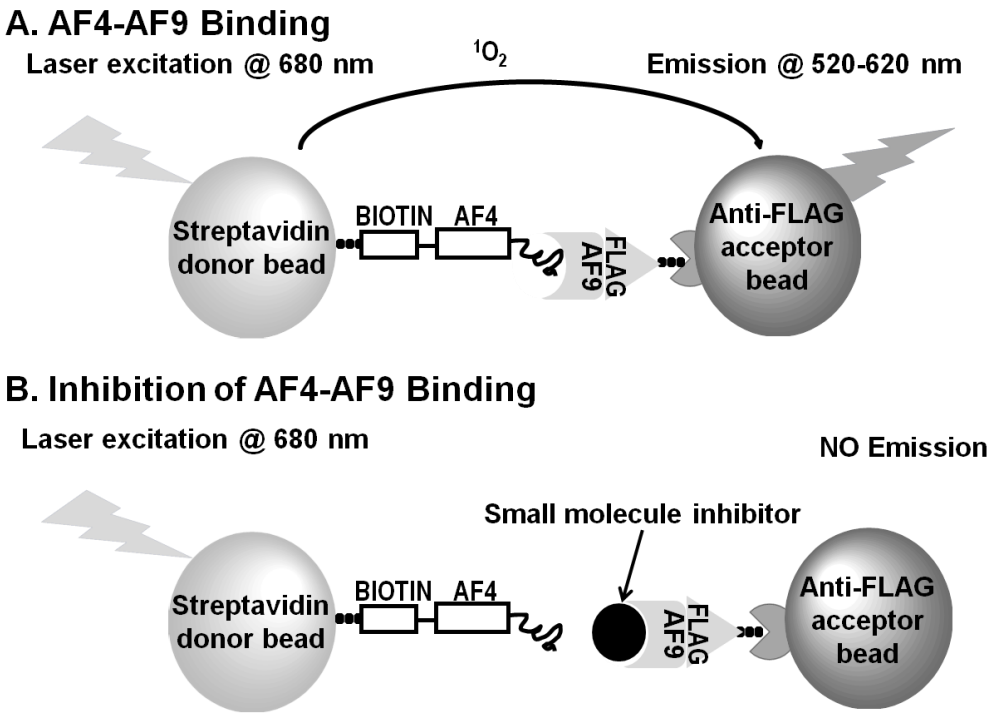

Fig. 2.1. AlphaScreen assay to screen for inhibitors of AF4-AF9 binding. (A) The protein-peptide interaction is detected by AlphaScreen upon the addition of streptavidin coated donor beads and anti-FLAG-coated acceptor beads. (B) A small

molecule inhibitor can be identified by decreased signal due to disruption of protein-peptide binding by the inhibitor.

The step-by-step protocol that I used for HTS was developed and optimized before I joined the group by Kathy Drake and Venita Watson (Table 2.3). In the first step, 4 µL water containing 0.01% Tween-20 (or 4 µL 750 nM unlabeled AF4 27-mer for background wells of column 2 and 24) was added into white 384-well AlphaPlates SW, followed by pintool transfer of compounds in DMSO (column 3-22) or DMSO alone (column 1, 2, 23 and 24) from Nunc 384-well clear source plates containing 10 µL compound or DMSO per well. Then 3 µL of 8 nM biotin-AF4 27-mer peptide in 2.3X PBS buffer followed by 3 µL of 8 nM FLAG-AF9 in 1X PBS buffer was added, giving a final concentration of AF4 peptide and AF9 protein of 2.4 nM in 10 µL assay volume before bead addition. The plates were sealed during the first incubation period. Beads were premixed and added simultaneously in 1X buffer under subdued lighting after 90 minutes incubation. Plates were sealed again during the second incubation period of 60 minutes, after which luminescence was read on an EnVision plate reader.

Table 2.3. HTS protocol

Step	Parameter	Value	Description
1	Water/0.01% Tween-20	4 µL	Add to 384-well plate
2[a]	Compound in DMSO	50 nL	Pintool transfer compound into water
3	Biotin-AF4 27-mer peptide	3 µL	Tip transfer on JANUS MDT
4[b]	AF9-FLAG	3 µL	Tip transfer on JANUS MDT
5	Incubation time	90 min	At room temperature
6	1:1 Anti-FLAG beads/Streptavidin	2 µL	Tip transfer on JANUS MDT
7	Incubation time	60 min	Plates maintained in low light at room temperature
8	AlphaScreen readout	cps	Perkin Elmer EnVision® multilabel reader with standard AlphaScreen option (Em = 570 nm)

[a] Pintool transferred compound from source plate always containing 10 µL compound in DMSO per well.

[b] AF9 is a highly disorganized protein prone to aggregation. It is added last because it is stabilized by binding to AF4.

2.2.2 Dose-response and Counterscreen

Activity of HTS hits was confirmed by determination of potency by dose-response, in which inhibitors were serially diluted and tested in the AF4-AF9 binding assay following the protocol described in *Table 2.3*. For TimTec, Microsource, and Broad Institute collections screening, hits were re-ordered as solids and dissolved in DMSO to make 40 mM stock. Then half-diluted the stock solution from 40 mM down to 1.22 µM, giving the final concentration in 10 µL from 200 µM to 6.1 nM. For

LCGC collection screening, hits were re-ordered as solutions of 10 mM or 1.25 mM in DMSO, then these stock solutions were two-fold serial diluted down to 0.3 µM or 0.038 µM, giving a final concentration in 10 µL from 50 µM to 1.5 nM or from 6.25 µM to 0.19 nM. Data was fit to obtain IC_{50} value as described under Data Analysis.

To eliminate false positives interfering with either AlphaScreen signal generation or bead capture, HTS hits were tested in a counterscreen in parallel with dose-response testing in the AF4-AF9 binding assay. Compounds were tested in dose-response using a biotin–FLAG peptide in place of biotin-AF4 27-mer and AF9-FLAG as the linker between anti-FLAG acceptor beads and streptavidin-coated donor beads (Fig. 2.2). Any compounds that caused a decrease in luminescence signal in the counterscreen as well as the binding assay were considered artifacts that were not directly disrupting AF4-AF9 binding. The same set of compounds that were serially diluted for dose–response confirmation in the AF4-AF9 binding assay were delivered by pintool and assayed in the counterscreen under identical conditions to the binding assay. In place of biotin-AF4 27-mer peptide and AF9, 6 µL of biotin–FLAG peptide in 1.67X assay buffer was added to give a final concentration of 7.5 nM in 10 µL. This concentration provided a signal equivalent to the highest signal observed for the AF4-AF9 assay. Control (100% signal, column 1 & 23) comprised 7.5nM biotin-FLAG in the absence of compounds; for the background (0% signal, column 2 & 24), the buffer was substituted for biotin–FLAG.

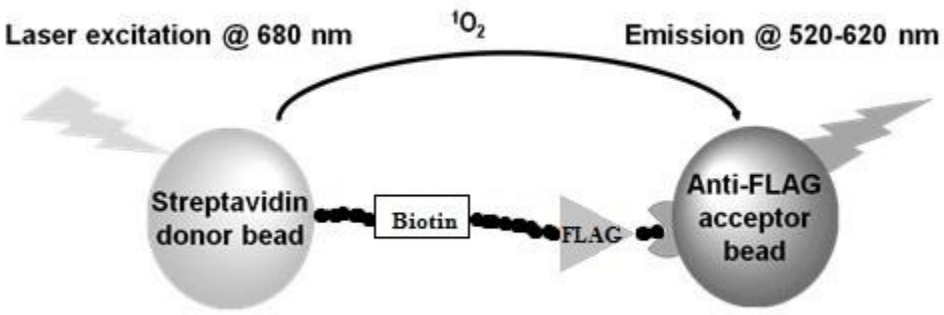

Fig. 2.2. Biotin-FLAG counterscreen. Biotin-AF4 27-mer and AF9-FLAG are replaced by Biotin-FLAG in counterscreen.

2.2.3 Data Analysis

2.2.3.1 HTS Hit Identification

For non-pooled library screening, AlphaScreen signals were converted to percent inhibition with *Eq. 1*. Hit was identified as compounds giving an AlphaScreen signal >3 SD below the mean control signal obtained in the absence of test compound.

$$\text{Percent inhibition} = 100 - \text{percent activity} \quad (1)$$

For orthogonally pooled libraries, the HTS procedure and the percent inhibition data analysis were the same as for non-pooled library screening. However, since the orthogonally pooled library comprised a 10-compound mixture in each well, and each compound was located in two locations of two different plates, the percent inhibition in the two wells containing each compound had to be compared to identify active compounds (Fig. 2.3). A macro-enabled Excel template (CeuticalSoft, Hudson, NY) was used to identify the hits from the orthogonally pooled library. Taking *Fig. 2.3* as an example, compound X shown as a black square in well 18 of plate C7 is pooled into mixture plates M-7 and M-C. So well 18 of both plates M-7 and M-C will

contain compound X mixed with 9 other compounds. If, after analysis of HTS results using the macro-enabled Excel template, the percent inhibition from well 18 of mixture plates M-7 and M-C both pass the 3 SD cutoff, compound X can be identified as the active component in both wells and selected as a hit (Fig. 3.8).

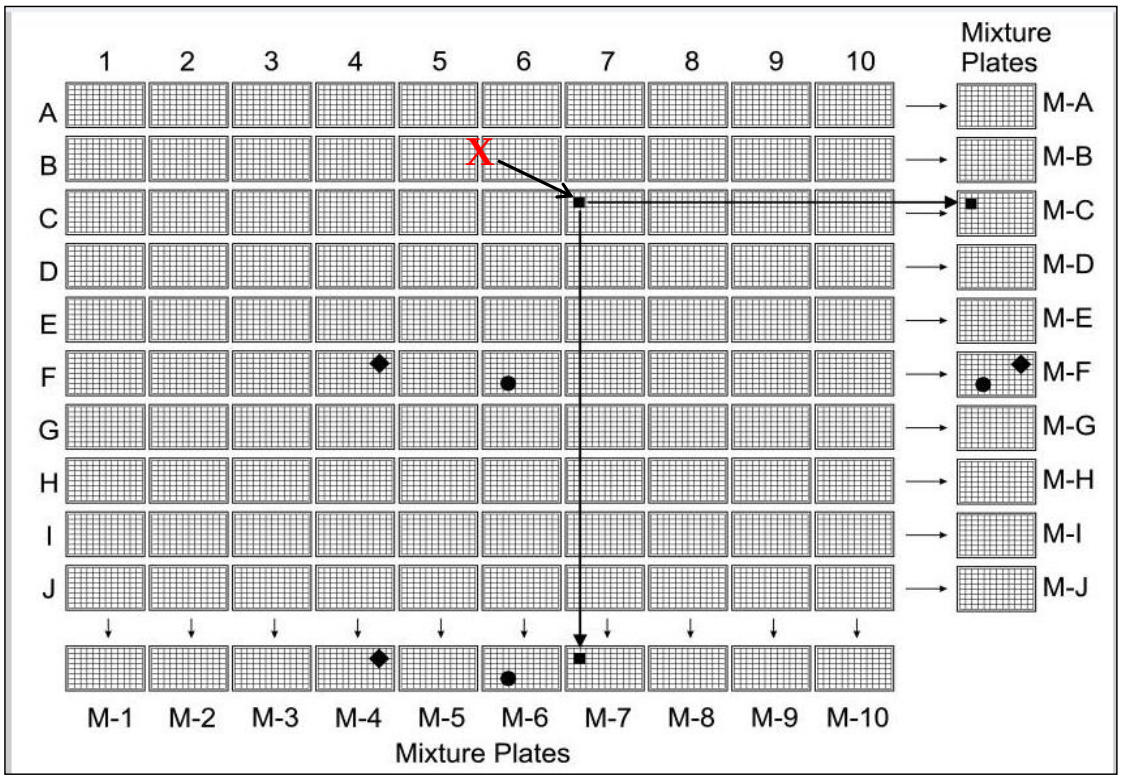

Fig. 2.3. Illustration of orthogonal pooling [23]. 100 384-well plates (A1-J10) are pooled into 20 mixture plates (M-1 to M-10, M-A to M-J). Black dots represent the locations of the 3 different compounds before and after the orthogonal pooling. Note how each compound is in two locations in the mixture plates.

2.2.3.2 Dose–response Analysis

AlphaScreen signals were converted to percent activity (Eq. 2) for dose–response data analysis. Data were fit by *log(inhibition) vs. response-Variable slope* equation in GraphPad Prism.

$$\text{Percent activity} = 100 \times \left(\frac{\text{CPS}_{\text{compound}} - \text{CPS}_{\text{AVG background}}}{\text{CPS}_{\text{AVG control}} - \text{CPS}_{\text{AVG background}}}\right) \quad (2)$$

2.2.3.3 Signal/Background and Z'-factor

The Signal/Background (Eq. 3) and Z'-factor (Eq. 4), two important statistical indicators to monitor the quality of the HTS assay, were determined using equations previously described [24].

$$\frac{\text{S}}{\text{B}} = \frac{\text{CPS}_{\text{AVG control}}}{\text{CPS}_{\text{AVG background}}} \quad (3)$$

$$\text{Z}' - \text{factor} = 1 - \frac{3 \times (\sigma_{\text{AVG control}} - \sigma_{\text{AVG background}})}{(\mu_{\text{AVG control}} - \mu_{\text{AVG background}})} \quad (4)$$

where μ and σ represent the mean and standard deviation, respectively.

2.3 ChemBridge Collection Screen

2.3.1 Compound Compression

The ChemBridge library comprises 100,000 compounds in 1,250 Corning Costar V-bottom 96-well plates with 100 μL per well. Each four 96-well plates were compressed into one Nunc clear plate, thereby compressing the library into a total of 313 384-well plates. 20 μL compound was transferred from each well of 96-well plate into a Nunc 384-well clear plate as shown in *Fig. 2.4*. Then 10 μL was transferred from each well of each of the 313 Nunc 384-well clear plate to another Nunc 384-well clear plate to make a copy. The transfer and wash procedures were the same as described above.

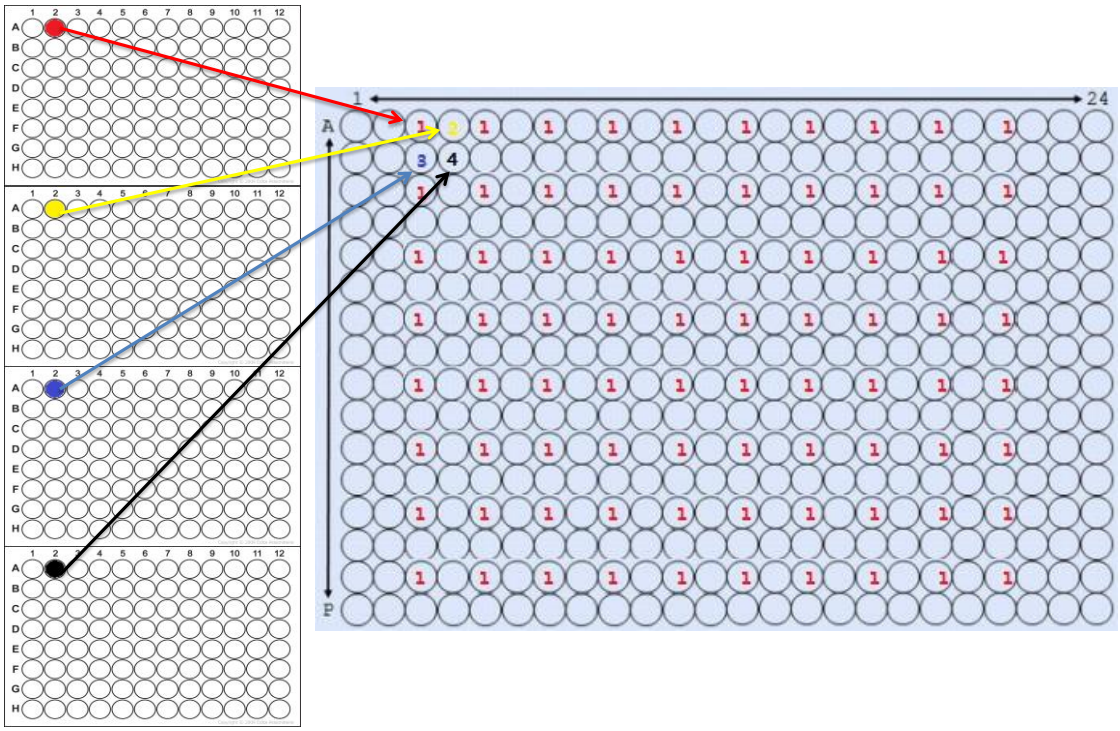

Fig. 2.4. Compound compression. Four 96-well plates containing 80 compounds each were compressed into one 384-well plate. The compounds from the 1st, 2nd, 3rd, and 4th 96-well plate were reformatted into quadrant 1, 2, 3, and 4 of the 384-well plate, respectively.

2.3.1.1 Tip Transfer Validation

Tips were pre-washed with the tip wash procedure described above. Fluorescein sodium salt was dissolved in DMSO to make 100 µL of a 200 nM solution in each well of a Nunc 384-well clear source plate. Using the tip transfer procedure described in *Section 2.2.2.1,* 20 µL fluorescein was transferred from the source plate to a 384-well black plate, the wells of the source plate were refilled to 100 µL of 200 nM fluorescein solution after the transfer, and the tips were washed using the tip wash procedure. Fluorescein was transferred into 3 different Nunc 384-well black plates and the plates were read on an EnVision plate reader. A 15-point serial dilution of 800

nM Fluorescein in DMSO was used to generate a standard curve, which was used to convert measured fluorescein fluorescence after tip transfer to μL transferred volume.

2.3.1.2 Tip Carryover Validation

Tips were pre-washed with the tip wash procedure described above. Fluorescein sodium salt was dissolved in DMSO to make 100 μL of 200 μM solution in each well of a Nunc 384-well clear source plate. Using the tip transfer procedure described above, 20 μL fluorescein was transferred from source plate to Nunc 384-well black plate, the wells of the source plate were refilled to 100 μL of 200 nM fluorescein solution after the transfer, and the tips were washed using the tip wash procedure. Tip transfer and washing was repeated 10 times, using a new Nunc 384-well black plate for each transfer. After the 10th transfer, 100 μL per well of 200 nM fluorescein solution in the source plate was replaced by 100 μL DMSO. Then 20 μL DMSO was transferred to each well of a new Nunc 384-well black plate. The whole process was repeated 3 times to obtain results from 3 different Nunc 384-well black plates. 800 nM fluorescein in DMSO was serial diluted 15 times to make a standard curve, and this curve was used to convert signal to volume carried over.

2.3.2 Orthogonal Pooling

2.3.2.1 Tip Transfer Validation

Tips were pre-washed with the tip wash procedure. Fluorescein sodium salt was dissolved in DMSO to make 10 μL of 5 μM solution in each well of a Nunc 384-well clear source plate. Using the tip transfer procedure, 2 μL of fluorescein was transferred from source plate to a Nunc 384-well black plate, followed by the tip wash procedure. Addition of 8 μL DMSO and 90 μL NaOH, pH 9, was used to amplify the

signal, which was read on an EnVision plate reader. A 15-point serial dilution of 800 nM fluorescein DMSO was used to generate a standard curve. Signal was converted to µL transferred volume using the standard curve.

2.4 LCGC Collection Screen

2.4.1 Pintool Transfer Validation

The pintool was soaked in 110 mL 1X VP110 Pin Cleaning Solution (V & P Scientific, San Diego, CA) for 30 minutes, and then washed according to the pintool wash procedure as described in *Table 2.3 B*. Fluorescein sodium salt was dissolved in DMSO to make 10 µL of a 40 µM solution in each well of a Nunc 384-well clear source plate. This solution of fluorescein was transferred by pintool from the source plate into a 384-well white AlphaScreen SW containing 4 µL water and 0.01% Tween-20, after which the pintool was washed according to the pintool wash procedure. The transfer was repeated three times and the three white AlphaScreen SW were read on an EnVision plate reader. A standard curve was generated by 15-step serial dilution of 800 nM fluorescein in DMSO. Signal was converted to nL transferred volume using the standard curve.

2.4.2 Pintool Carryover Validation

Fluorescein was transferred by pintool as described in *Section 2.4.1*. The transfer was repeated 10 times, in each case into a new white AlphaScreen SW. After the 10 transfers of fluorescein, the pintool was used to transfer DMSO from a Nunc 384-well clear source plate containing 10 µL DMSO per well into a white AlphaScreen SW plate containing 4 µL water and 0.01% Tween-20 and this was also

read on the EnVision plate reader. Signal was converted to volume of fluorescein carried over using a standard curve generated as in *Section 2.4.1*.

2.5 Hit Optimization

Several compound libraries have been tested using the AF4-AF9 binding assay described in this thesis. The Micosource and TimTec libraries were screened by Kathy Drake and Venita Watson, after which I retested solid samples of each active compound and characterized analogs of anabasine, the most promising hit from the pilot screen. Analogs of the most promising hit TV040365 from the Broad Institute library were also tested.

2.5.1 Ki Determination of Anabasine, Broad Institute Compound TV040365 and AF4 12-mer in Triplicate.

The same Ki determination procedure was used for anabasine and TV040365. Row A of aNunc 384-well clear source plate contained 10 µL per well of 10 mM anabasine in DMSO. The 10 mM anabasine stock in Row A was 2/3-fold serial diluted down to 1.3 mM anabasine in Row F. Rows G and H contained only 10 µL DMSO per well. 4 µL water/Tween-20 was added into Rows A to G of a white AlphaScreen SW plate, and 4 µL water/Tween-20 containing 750 nM AF4 27-mer was added to Row H. Anabasine was transferred by pintool from the source plate to the white AlphaScreen SW plate, and 3 µL of 32 nM biotin-AF4 27-mer in 2.3X PBS buffer was added to Columns 1, 2 and 3 of the white AlphaScreen SW plate. Two-fold serial dilutions of biotin-AF4 27-mer were then added as follows: A stock of 32 nM biotin-AF4 27-mer was two-fold diluted to 16 nM and 3 µL of the 16 nM solution was added to Columns 4, 5 and 6; following two-fold dilution of the 16 nM biotin-AF4 27-mer to 8 nM, 3 µL of the 8 nM solution was added to the next three columns (7, 8 and 9). Two-fold

dilution and addition was repeated until 3 µL of 0.5 nM biotin-AF4 27-mer was added to Columns 19, 20 and 21. Then 3 µL of 2.3X PBS buffer was added to Columns 22, 23 and 24, followed by the addition of 3 µL of 0.4 nM AF9-FLAG and 2 µL of 120 mg/mL 1:1 anti-FLAG acceptor and streptavidin donor beads to all wells from Row A to Row H. The plate was read on an EnVision plate reader and data were fit using the *Competitive inhibition, Uncompetitive inhibition, and Noncompetitive inhibition* equations in GraphPad Prism.

The same procedure was used for determination of the Ki of the AF4 12-mer peptide, except the Nunc 384-well clear source plate contained two-fold serial dilution of AF4 12-mer from 8 µM in Row A down to 250 nM in Row F.

Chapter 3

RESULTS

3.1 Assay Validation

3.1.1 Competition Experiments with Non-biotinylated AF4

To demonstrate specificity and reversibility of AF4 peptide binding to AF9, a competition binding assay with non-biotinylated peptides of varying lengths was performed by Kathy Drake and Venita Watson (Fig. 3.1). Non-biotinylated AF4 27-mer effectively competed with biotin-AF4 27-mer. Applying a sigmoidal dose-response model gave an IC_{50} of 2.7 nM. As the length of the non-biotinylated AF4 peptide decreased, the IC_{50} increased: a 12-mer peptide gave an IC_{50} of 5.8 nM, a 10-mer peptide gave an IC_{50} of 13.2 nM, whereas truncating the sequence to 8 amino acids abolished activity entirely. Changing only two residues of the 12-amino acid peptide also completely abolished activity [20]. This potency ranking correlates well with the data reported by Hemenway et al. [16].

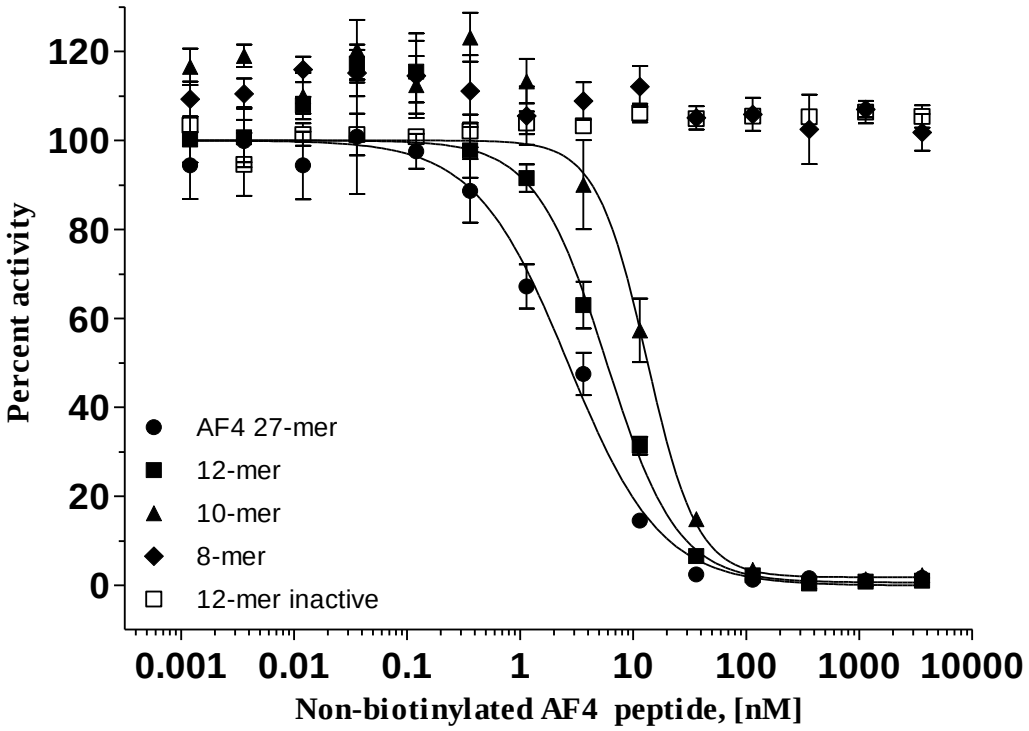

Fig. 3.1. Competition of non-biotinylated AF4 peptides with biotin-AF4 27-mer for binding to the AF9-FLAG protein. Non-biotinylated AF4 peptides of varying lengths were tested for inhibition of binding between biotin-AF4 27-mer peptide and AF9-FLAG. The unlabeled peptides in order of potency were AF4 27-mer (●), 12-mer (■), and 10-mer (▲). The 8-mer (◆) and 12-mer (inactive sequence) (□) showed no inhibition of binding. Values = mean ± SEM; n = 3.

3.1.2 Validation of HTS Liquid Handling for ChemBridge Library Compression and Orthogonal Pooling

The validation of 20 µL transfer (Table 3.1, Fig. 3.2) was performed in triplicate. The average transfer volumes in the three plates were all close to 21 µL. One outlier from plate 1 showed the lowest transfer volume at 13.08 µL. For the validation of carryover after 10 transfers (Fig. 3.3), the values were expressed as transferred volume of 200 µM fluorescein sodium salt in DMSO. The average percent carryovers for three plates were all lower than 0.15%. The transfer and carryover

validations showed constant and precise results, which met the requirements for consistent plate compression and compound pooling.

Table 3.1. Statistics of 20 µL transfer validation with P30 tips

Transfer (µL)	Plate 1	Plate 2	Plate 3
Number of values	96	96	96
Minimum	13.08	18.83	19.16
Maximum	34.65	25.58	26.27
Mean	21.43	21.93	21.85
SD	1.39	1.25	1.21

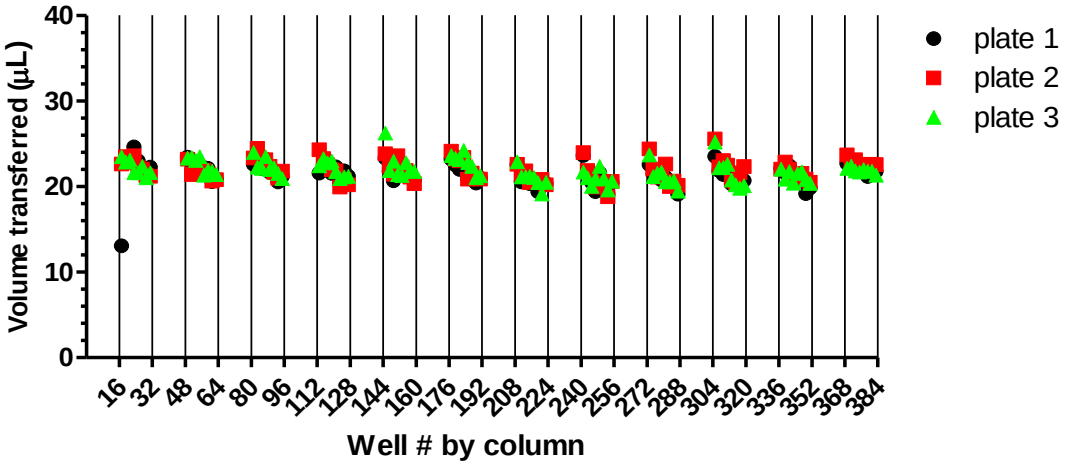

Fig. 3.2. Transfer validation results expressed as transfer volume vs. well number by column. 20 µL DMSO contained 200 nM fluorescein sodium salt was transferred by 96 P30 tips from a Nunc 384-well clear plate to a Nunc 384-well black plates. Plates were read on an Envision Plate Reader. Signal was converted to volume using a standard curve.

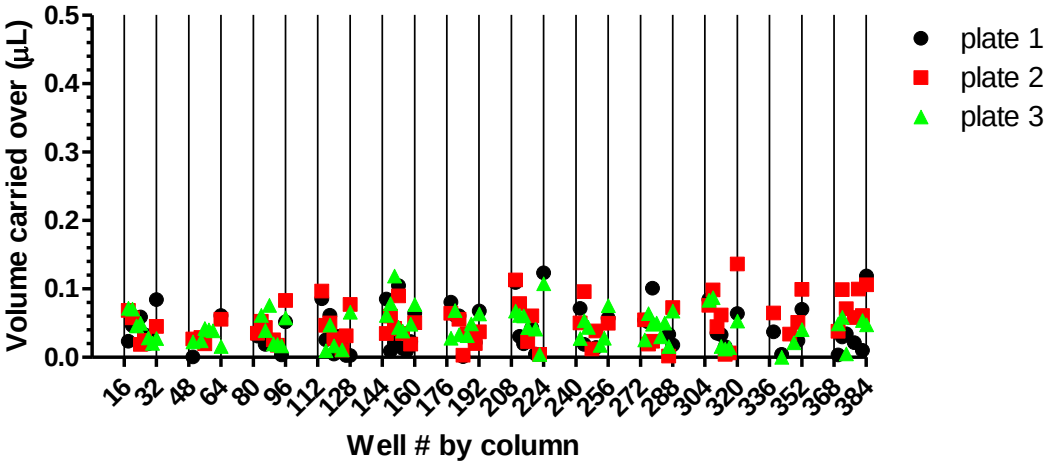

Fig. 3.3. Carryover validation results expressed by volume carried over vs. well number by column. For each transfer, 20 µL of a solution of 200 µM fluorescein sodium salt in DMSO was aspirated by P30 tips from a Nunc 384-well clear plate, and dispensed into Nunc 384-well clear plates, followed by tip wash procedure. After the 10th transfer, 20 µL DMSO (without added fluorescein sodium salt) was transferred using the same tips to a Nunc 384-well black plates to determine carryover. Plates were read on an Envision Plate Reader. Signal was converted to volume using a standard curve.

The 2 µL transfer volume required for orthogonal pooling was validated using a solution of fluorescein sodium salt in DMSO (Fig. 3.4). Data was generated from 352 P30 tips. The mean transfer volume was 2.1510 µL and the range was from 2.0015 µL to 2.3088 µL. These validation results indicated that a volume as low as 2 μL could be transferred using P30 tips with low variability and high precision.

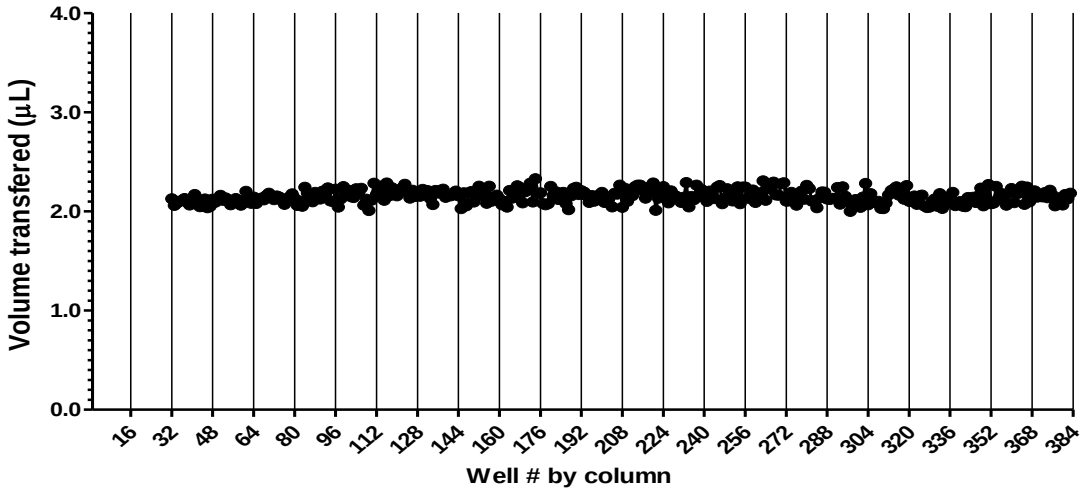

Fig. 3.4. Validation of low volume transfer with P30 tips. Data was generated from 352 P30 tips by transferring 2 µL of 5 µM fluorescein sodium salt in DMSO from a Nunc 384-well clear plate to a Nunc 384-well black plate, and diluting 50-fold with NaOH, pH 9, before reading fluorescence on an EnVision plate reader.

3.1.3 Validation of HTS Liquid Handling for LCGC Library

Validations of the precision of pintool transfer and confirmation of the lack of carryover were done before the screen of the LCGC compound library. The transfer validation was done by triplicate (Table 3.2, Fig. 3.5), giving an average pintool transfer volume close to 50 nL. The low CV (coefficient variance) indicated a consistant transfer volume. The percent carryover on each of 384 pins after 10 transfers (Fig. 3.6) ranged from 0.001% to 0.103%. One outlier showed 0.319 nL (0.638%) carryover. The average and standard deviation of the percent carryover were 0.026% and 0.034%, respectively.

Table 3.2. Statistics of pintool transfer validation

Transfer (nL)	Plate 1	Plate 2	Plate 3
Number of values	384	384	384
Minimum	37.1	37.4	41.3
Maximum	62.8	65.4	72.2
Mean	49.2	49.4	55.9
SD	4.88	4.8	6.09

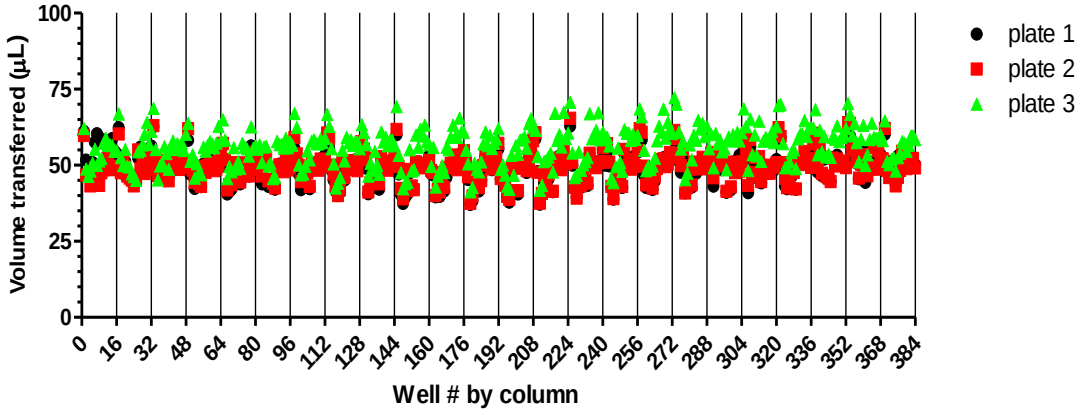

Fig. 3.5. Pintool transfer validation. The graph shows volume transferred vs. well number by column. Pintool transfer was from a Nunc 384-well clear plate containing 10 µL of 40 µM fluorescein sodium salt to a white AlphaScreen SW plate containing 4 µL 0.01% Tween-20. Plates were read on an EnVision Plate Reader. Signal was converted to volume using a standard curve.

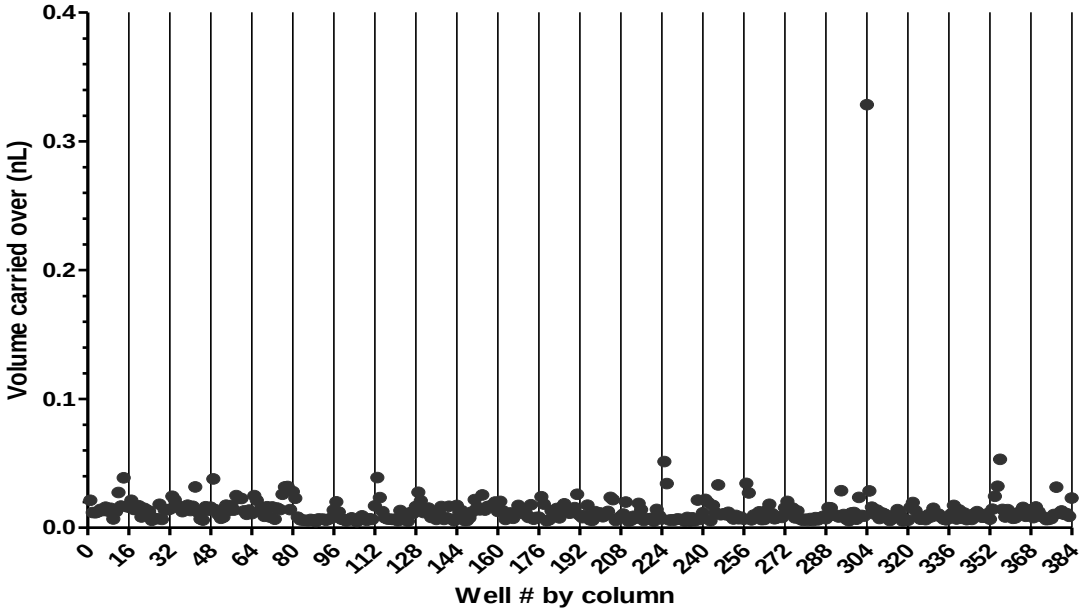

Fig. 3.6. Pintool carryover validation after 10 transfers. Pintool transfer was from a Nunc 384-well clear source plate containing 10 µL of 10 mM fluorescein sodium salt in DMSO into a white AlphaScreen SW plate containing 4 µL of 0.01% Tween-20. The pintool wash procedure was performed after each transfer. To determine carryover after the 10th transfer, DMSO (without added fluorescein sodium salt) was transferred from a Nunc 384-well clear plate to a white AlphaPlate SW plate containing 4 µL 0.01% Tween-20. Plates were read on an EnVision Plate Reader. Signal was converted to volume using a standard curve.

3.2 Compression and Orthogonal Pooling of ChemBridge Library

The ChemBridge library comprising 100,000 compounds in 1,250 Costar 96-well clear v-bottom plates containing a single compound in 100 µL per well with a concentration at 10 mM were compressed into 313 Nunc 384-well clear plates to give 20 µL/well (Fig. 2.4). A copy containing 10 µL per well was made from each compressed plate.

To generate an orthogonally pooled layout of the library, every 100 compressed plates were pooled into 20 mixture plates (Fig. 2.3). Therefore, 313 384-well compressed plates were pooled into 60 mixture plates, leaving 13 compressed

plates not pooled. Each mixture plate contained 20 µL/well of a mixture of 10 compounds at a final concentration of 1 mM for each compound. The remaining 13 compressed plates that were not pooled contained a single compound per well at a 10 mM concentration in 10 µL.

3.3 Screen of LCGC Collection

96,000 compounds in 60 orthogonally pooled Nunc 384-well clear plates received from the Lankenau Chemical Genomics Center (Wynnewood, PA) were screened at a compound concentration of 0.78 µM or 1.56 µM, depending on the concentration of each source plate. The HTS protocol was carried out as described in *Table 2.3*. The screen was finished in 5 days (12 plates per day with 4 QC plates). AlphaScreen signal was converted to percent inhibition using *Eq. 2* and percent inhibition of each compound mixture was analyzed by macro-enabled template as described in *Section 2.2.3.1*.

The screen statistics (Fig. 3.7) reveals CVs for the controls were fairly consistent, and they were all lower than 10%, except for one outlier of 12.4% in plate 44. The Z'-factors for the 60 screen plates were all higher than 0.7, which indicated a robust assay [24].

A

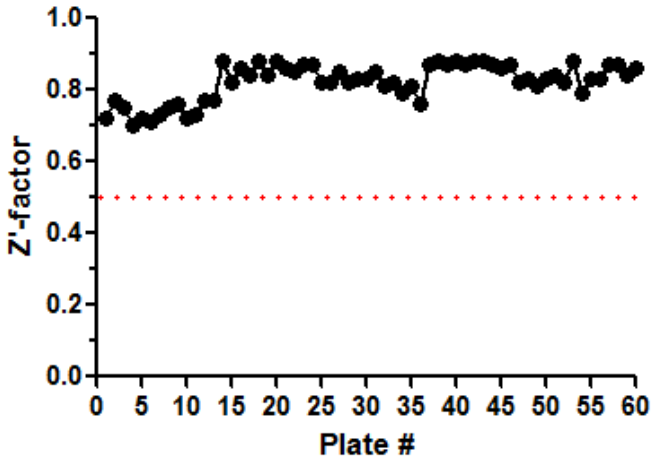

B

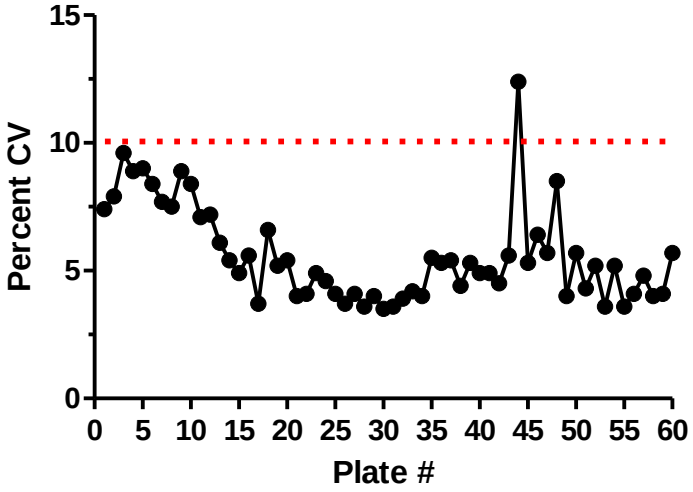

Fig. 3.7. Z'-factor and CV results of 60 LCGC screen plates. (A) The Z'-factors of the 60 screen plates were all higher than 0.6, giving an average of approximately 0.8. The red dashed line represents a Z'-factor = 0.5. Z'-factor > 0.5 indicates a robust assay. (B) CV was calculated as *SD of control/Mean of control*. All screen plates showed lower than 10% CV. The red dash line represents 10% CV. One outlier, plate 44, had more than 10% CV.

3.4 Identify LCGC Hits with Macro-enabled Template.

To identify the hits, three times the SD of the controls in each screen plate was used as cutoff. This is because random scatter of the controls and inactive compounds follows a Normal distribution, hence data differing from the mean of the controls by greater than 3 SD o is unlikely to occur by chance and is likely to correspond to inhibition of the biological target. Since all 60 screen plates had low CVs and control SD close to 10%, we used a 30% as cutoff to identify hits for all the plates. Using the macro-enabled template, hits were classified as *Active*, *Ambiguou*s and *Orphan*. Each test compound was located in two wells with the same well number in different mixture plates (Fig 2.3). If both wells occupied by a specific compound X showed more than 30% inhibition and none of the other compounds sharing a well with compound X showed activity in their second location, then the compound X was classified as *Active* (Fig. 3.8). *Ambiguous* hits arose where compounds X and Y sharing an active well each also showed activity at their second location. Inhibition >30% was observed in the well containing both X and Y, and also in wells in two other plates, one containing X (but not Y) and one containing Y (but not X). In these cases it is likely that both X and Y are active hits, but this cannot be determined with certainty until X and Y are retested separately. An *Orphan* hit was defined as a compound that was active in one of its locations but not in the other. Apparent activity of Orphan hits usually does not confirm upon retest. Analysis of HTS results from the LCGC library gave 115 compounds identified as *Active*, 244 compounds identified as *Ambiguous*, and none as *Orphan*, representing an overall hit rate of 0.37%.

A

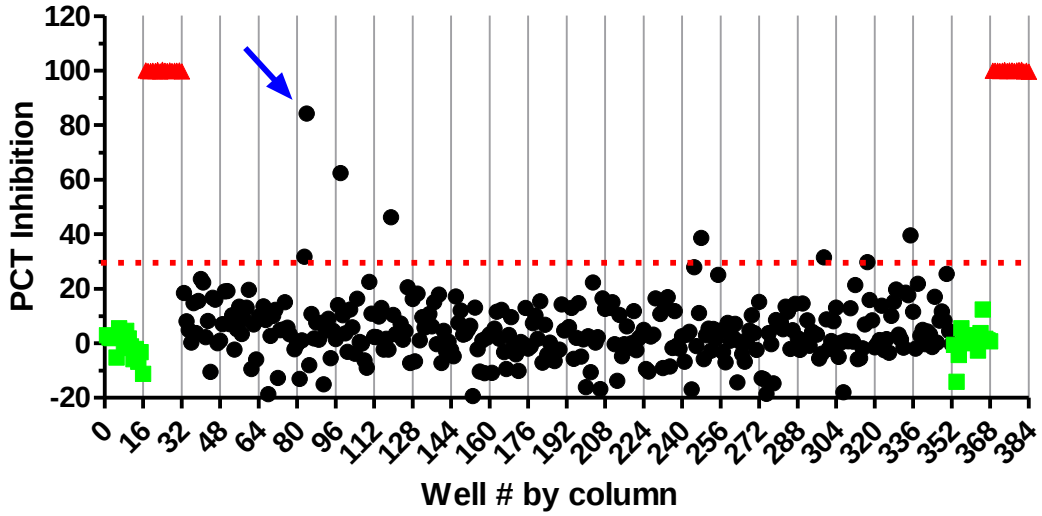

B

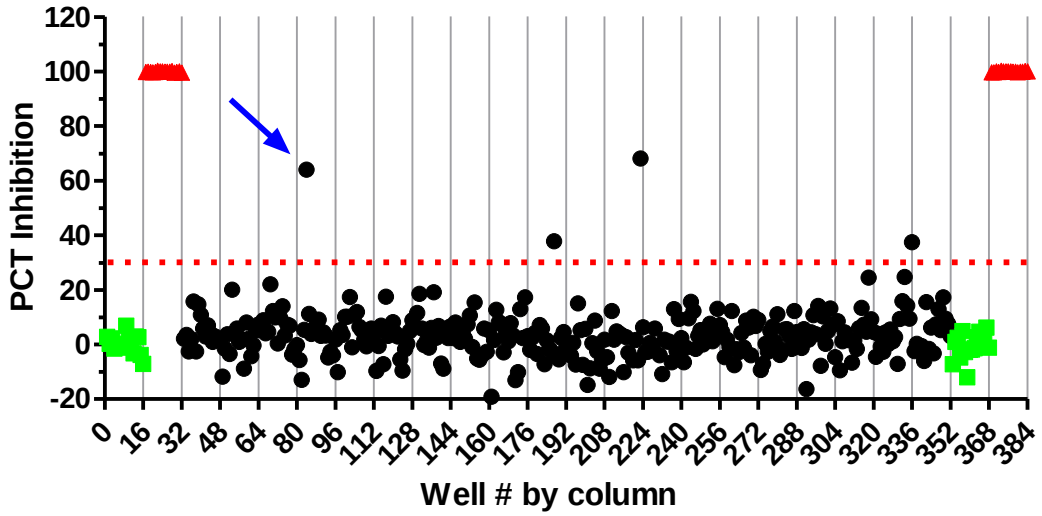

Fig. 3.8. Active hit identified by macro-enabled template. Panels A and B show data obtained from screening of two mixture plates from the LCGC library. The two black circles shown by blue arrows represent activity derived from a compound located in the same well (well 84) in two different mixture plates. Green squares, control; red triangles, background.

3.5 Confirmation of Hits with Dose-response Binding Assay and Counterscreen

Hits identified with macro-enabled template after primary screening were re-ordered as solutions in DMSO from the Lankenau Center for Chemical Genomics and were tested in triplicate in the AF4-AF9 binding assay and the counterscreen at a single concentration of 50 µM or 15.6 µM, depending on the concentration of each source plate. The 359 Active and Ambiguous compounds identified in the primary screen were retested at a single concentration in triplicate in the AF4-AF9 binding assay. Retesting confirmed 217 compounds as active in the binding assay. These were then tested at the same single concentration in the biotin-FLAG counterscreen, revealing 19 compounds that showed less inhibition in the counterscreen than in the binding assay (Fig 3.9). However, dose-response testing revealed that all the 19 hits were equally potent in both the AF4-AF9 binding assay and the counterscreen (Fig 3.10). Therefore, these compounds were considered artifacts that interfere with the assay and were not studied further.

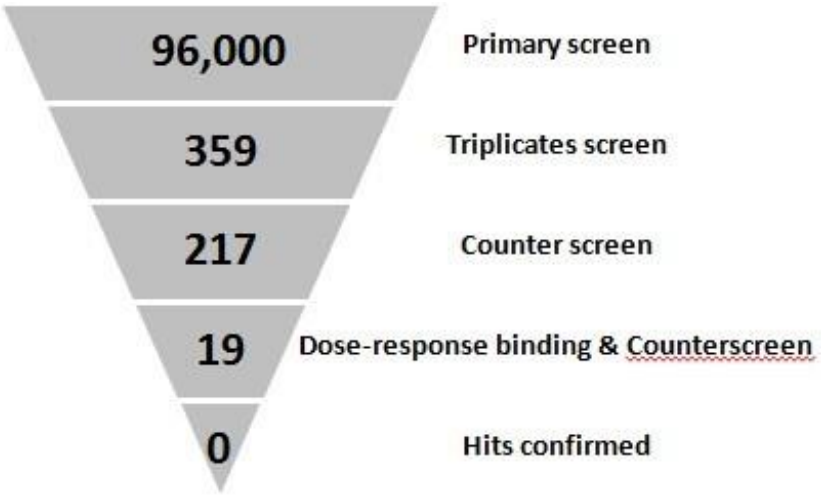

Fig. 3.9. Hit summary from LCGC screen. The LCGC library was screened using the AlphaScreen AF4-AF9 binding assay. After counterscreen and evaluation in dose-response, none of the hits were confirmed as selective for the binding assay.

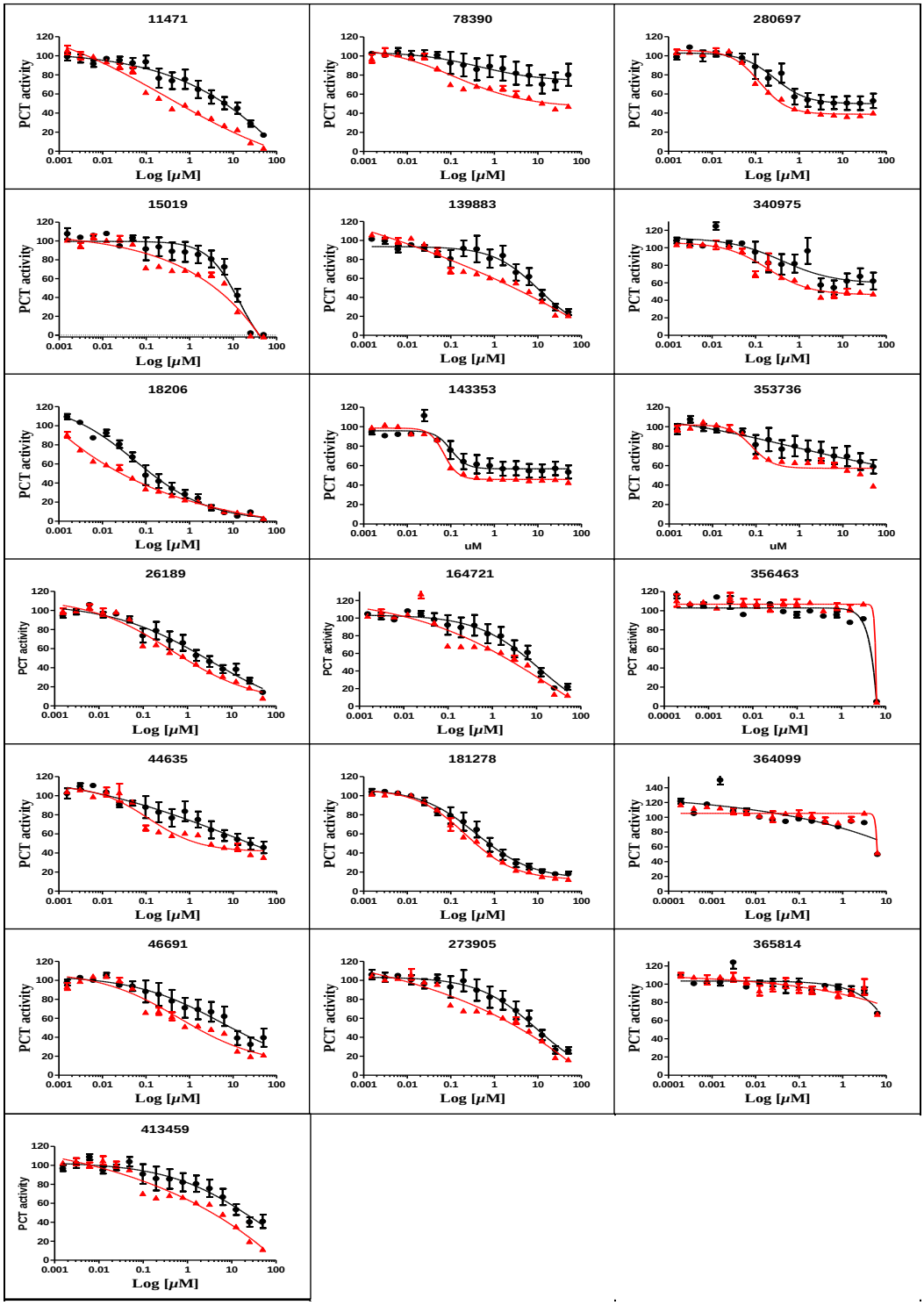

Fig. 3.10. Dose-response testing of LCGC hits in binding assay and counterscreen. Red curves represent dose-response binding assay with biotin-AF4 and AF9-FLAG. Black curves represent counterscreen with Biotin-FLAG.

3.6 Dose-response Confirmation of Hits from MicroSource Spectrum and TimTec Collection Screening

Pilot screening of the MicroSource spectrum and TimTec collections was done by Kathy Drake and Venita Watson before I joined the group. A total of 5,680 compounds were screened and 10 compounds were identified as active, representing a hit rate at 0.31%. The potency of these 10 hits was comfirmed by dose-response testing of fresh samples derived from dry powder in the AF4-AF9 binding assay and the biotin-FLAG counterscreen. Calculated IC_{50} values are shown in *Table 3.3* and dose-response curves in *Fig. 3.12*. Analysis of the data in *Table 3.3* and structures of the compounds (Figure 3.11) led to the choice of ST048429 (anabasine) for further study and optimization. This compound showed reasonable potency with an average IC_{50} of 12.2 μM and >16-fold selectivity for the binding assay over the counterscreen, and exhibited the most promising structure for chemical modification. Further study and optimization of this compound will be discussed later in this chapter. Three compounds gave higher potency and binding assay/counterscreen selectivity than anabasine, but their structures did not present an appealing scaffold for chemical modification, and analysis of screening data in the PubChem database showed these compounds to be active in many other screens [20]. Therefore, it is unlikely that these compounds could be optimized to selectively target the AF4-AF9 interaction in cells.

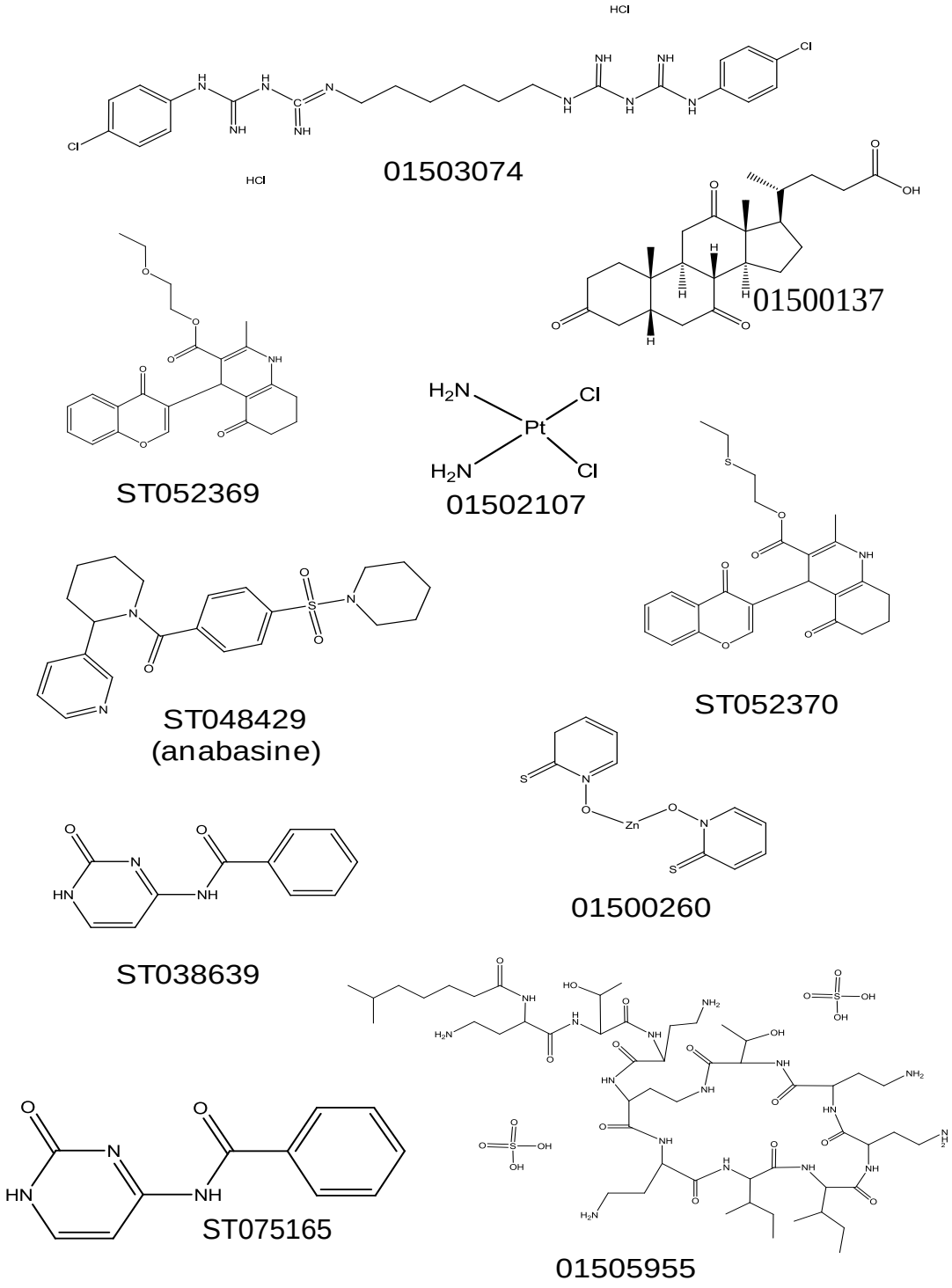

Fig. 3.11. Structures of pilot screening hits.

Table 3.3. Dose-response confirmation of MicroSource Spectrum and TimTec collection hits using solids

Compound ID	AF4-AF9 binding			Biotin-FLAG counterscreen			Selectivity (Counter IC_{50}/Binding IC_{50})
	IC_{50} (µM)	Mean IC_{50}	IC_{50} SD	IC_{50} (µM)	Mean IC_{50}	IC_{50} SD	
01503074	4.7			>200			
01503074	4.6	4.8	0.2	>200	>200		>40
01503074	5.0			>200			
01502107	5.7			>200			
01502107	4.9	5.2	0.4	>200	>200		>40
01502107	5.1			>200			
ST052370	9.3			>200			
ST052370	5.8	7.5	1.8	>200	>200		>30
ST052370	7.5			>200			
ST052369	12.0			>200			
ST052369	9.3	10.3	1.5	>200	>200		>20
ST052369	9.6			>200			
ST048429	14.8			>200			
ST048429	8.0	12.2	3.7	>200	>200		>16
ST048429	13.7			>200			
ST075165	30.5			>200			
ST075165	28.7	31.7	3.8	>200	>200		>7
ST075165	36.0			>200			
01500260	45.8			>200			
01500260	48.7	51.2		>200	>200		>4
01500260	59.2			>200			
01500137	100.1			>200			
01500137	209.8	138.8		>200	>200		>2
01500137	106.4			>200			
01505955	>200			>200			
01505955	>200	>200		>200	>200		Inactive
01505955	>200			>200			
ST038639	>200			>200			
ST038639	>200	>200		>200	>200		Inactive
ST038639	>200			>200			

Compound ID	Plate 1	Plate 2	Plate 3
01500137	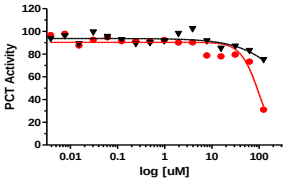	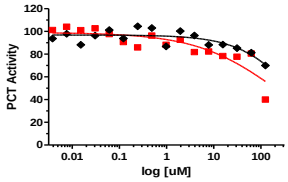	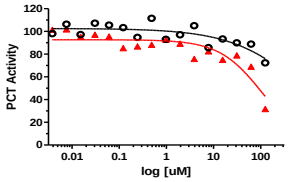
01500260	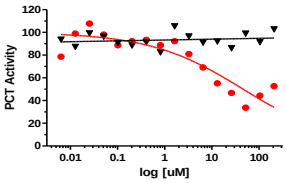	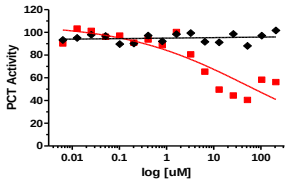	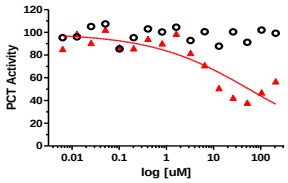
01502107	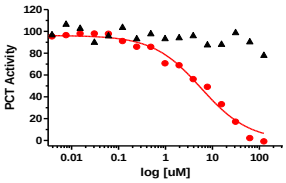	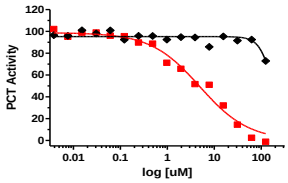	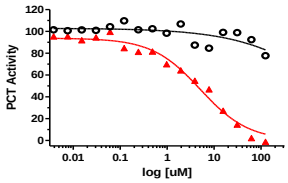
01503074	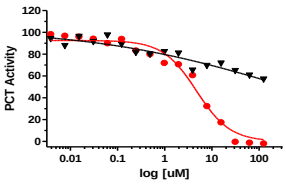	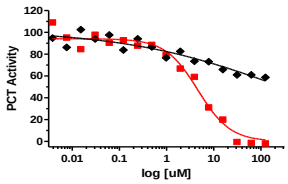	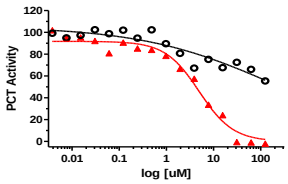
01505955	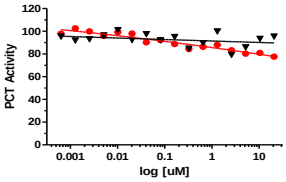	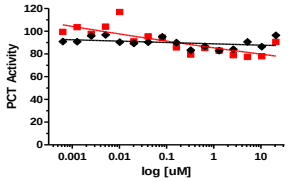	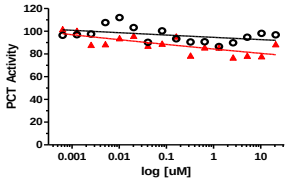

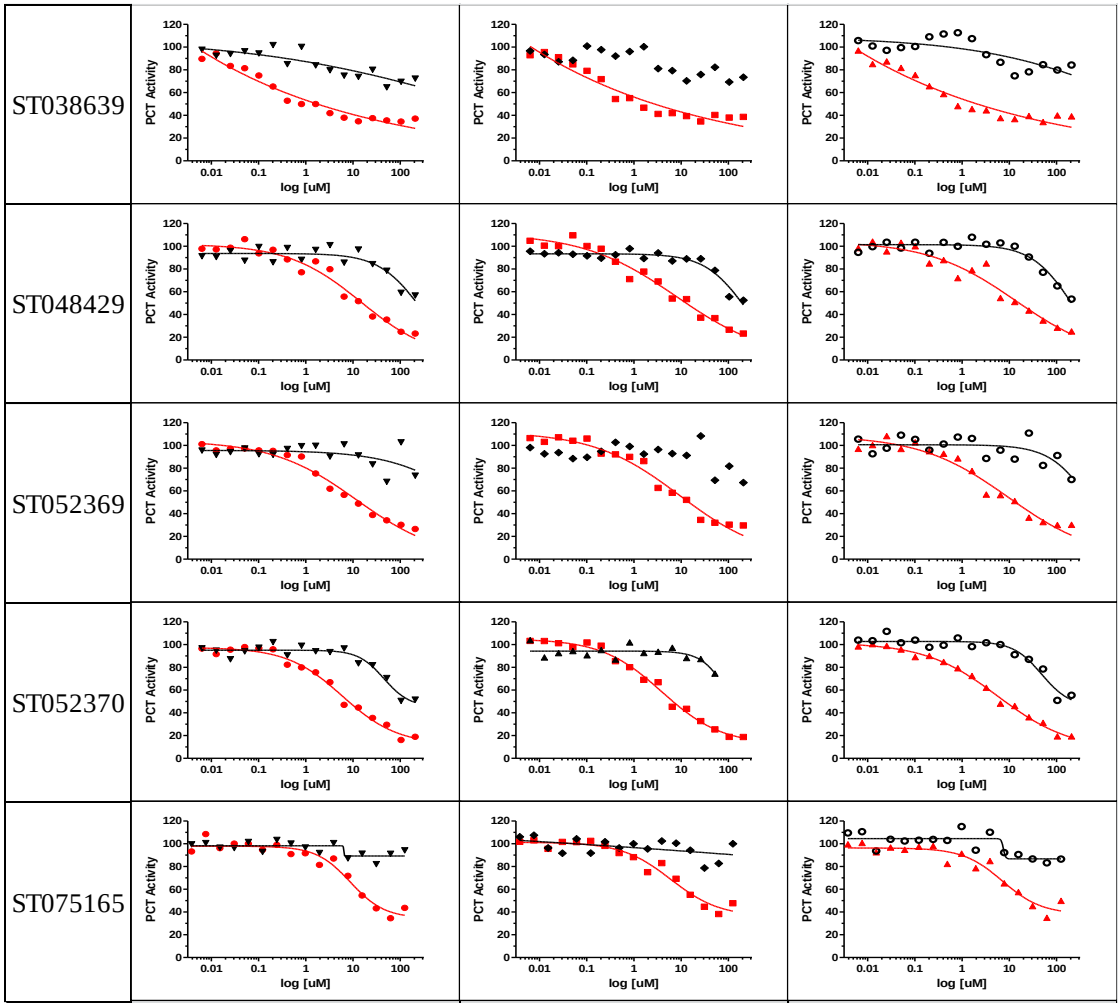

FIG. 3.12. Triplicate IC_{50} curves from dose-response testing of MicroSource spectrum and TimTec collection hits in binding assay and counterscreen. Red curves represent binding assay; black curves represent counterscreen.

3.7 Dose-response Confirmation of Hits from Broad Institute Screening

The AF4-AF9 binding assay developed by Kathy Drake and Venita Watson was transferred to the Broad Institute (Cambridge, MA) for screening of the 350,000-compound NIH compound library. Screening, counterscreen, and dose-response confirmation carried out at the Broad Institute led to 13 hits that showed greater potency in the binding assay than the counterscreen. Fresh powder samples of these

compounds were shipped from the Broad Institute and retested at Nemours in dose-response in the binding assay and counterscreen. Calculated IC_{50} values are shown in *Table 3.4*, dose-response curves in *Fig. 3.14*, and structures of the compounds in *Fig. 3.13*. Compared with the active compounds in *Table 3.3*, the hits from the Broad Institute screening showed much lower selectivity for the binding assay over the counterscreen. Two compounds were highly potent in the binding assay, but also exhibited similar activity in the counterscreen: TV040349 gave a mean IC_{50} of 80 nM in the binding assay, and TV040351 gave an IC_{50} of 180 nM, but both gave similar IC_{50} values of 70 nM and 100 nM, respectively, in the counterscreen. However, one compound TV040365 showed good selectivity for the binding assay and appeared amenable to chemical optimization.

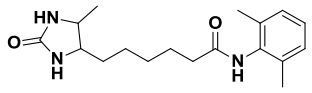

TV040347

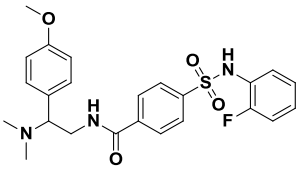

TV040353/4

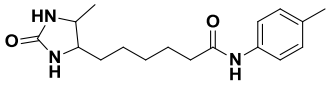

TV040349

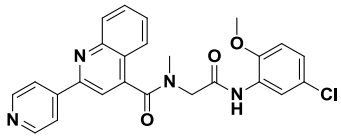

TV040355

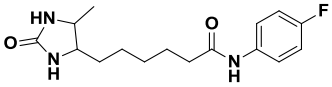

TV040351

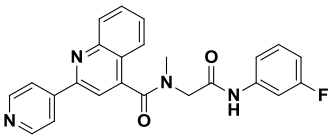

TV040357

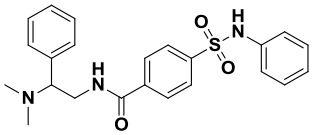

TV040359

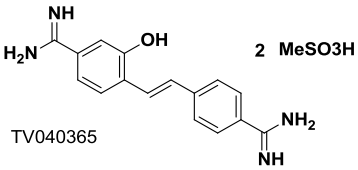

TV040365

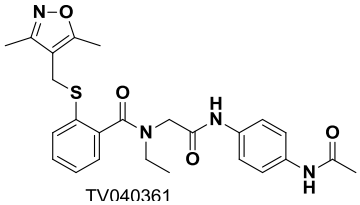

TV040361

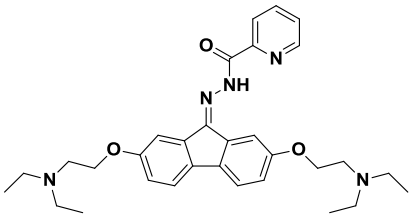

TV040367

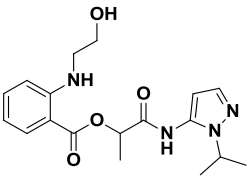

TV040363

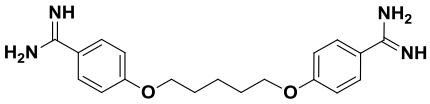

TV040369

Fig. 3.13. Structures of hits from Broad Institute screening

Table 3.4. Dose-response confirmation of hits from Broad Institute screening using solids

Compound ID	AF4-AF9 binding			Biotin-FLAG counterscreen			Selectivity (Counter IC_{50}/Binding IC_{50})
	IC_{50} (µM)	Mean IC_{50}	IC_{50} SD	IC_{50} (µM)	Mean IC_{50}	IC_{50} SD	
TV040365	28.03			>200			
TV040365	28.23	27.62	0.89	>200	>200		>7.2
TV040365	26.6			>200			
TV040367	51.5			311.9			
TV040367	77.03	69.70	15.86	211	244.17	58.66	3.50
TV040367	80.57			209.6			
TV040347	4.907			12.84			
TV040347	3.728	4.05	0.75	11.86	12.04	0.72	2.97
TV040347	3.521			11.43			
TV040361	121.6			>200			
TV040361	113.5	87.46	52.27	>200	>200		>2.3
TV040361	27.29			>200			
TV040349	0.07741			0.06699			
TV040349	0.08168	0.08	0.01	0.08154	0.07	0.01	0.85
TV040349	0.09055			0.06432			
TV040351	0.1568			0.0992			
TV040351	0.184	0.18	0.02	0.1136	0.10	0.01	0.58
TV040351	0.1918			0.09768			
TV040353	69.55			60.14			
TV040353	33.62	45.37	20.94	60.63	61.66	2.22	1.36
TV040353	32.95			64.21			
TV040343	>200			>200			
TV040343	>200	>200		>200	>200		Inactive
TV040343	>200			>200			
TV040355	29.36			>200			
TV040355	83.88	57.17	27.28	>200	>200		Inactive
TV040355	58.28			>200			
TV040357	>200			>200			
TV040357	>200	>200		>200	>200		Inactive
TV040357	>200			>200			
TV040359	>200			>200			
TV040359	>200	>200		>200	>200		Inactive
TV040359	>200			>200			
TV040363	>200			>200			
TV040363	>200	>200		>200	>200		Inactive
TV040363	>200			>200			
TV040369	>200			>200			
TV040369	>200	>200		>200	>200		Inactive
TV040369	>200			>200			

Compound ID	Plate 1	Plate 2	Plate 3
TV040343	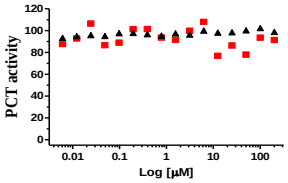	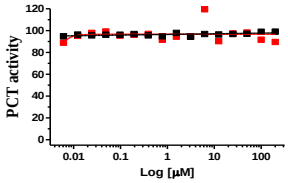	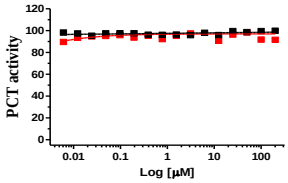
TV040347	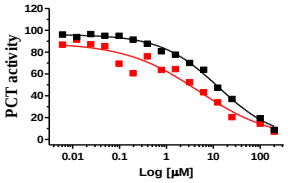	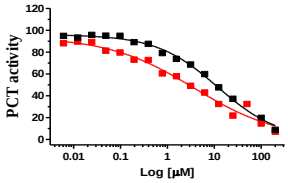	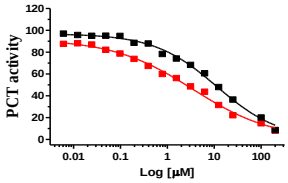
TV040349	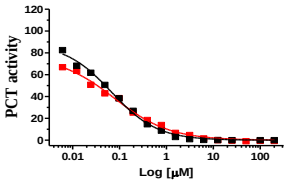	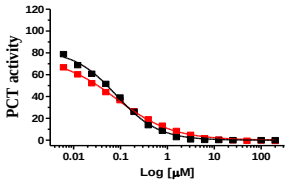	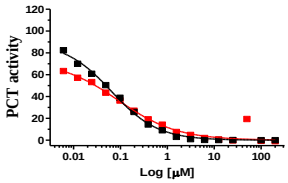
TV040351	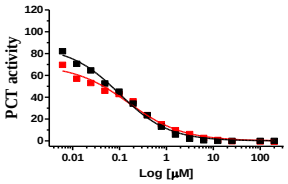	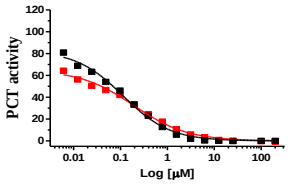	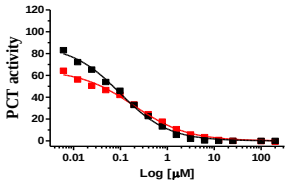
TV040353	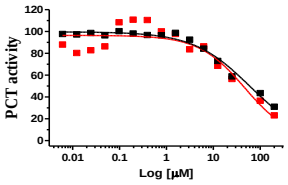	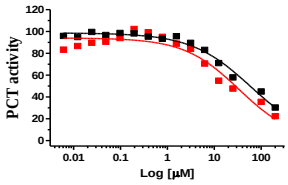	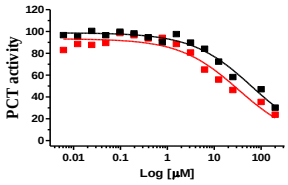
TV040355	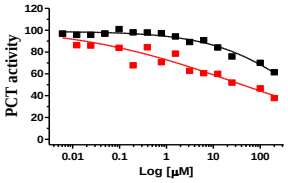	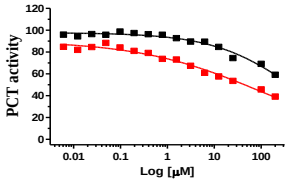	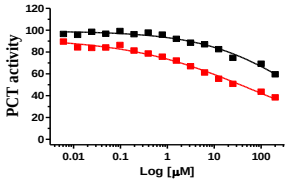
TV040357	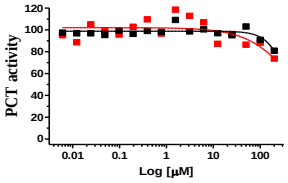	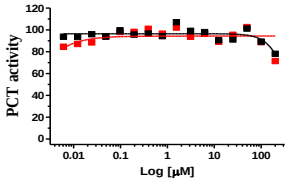	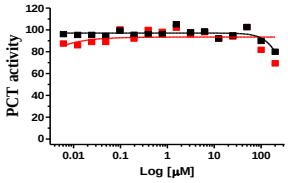

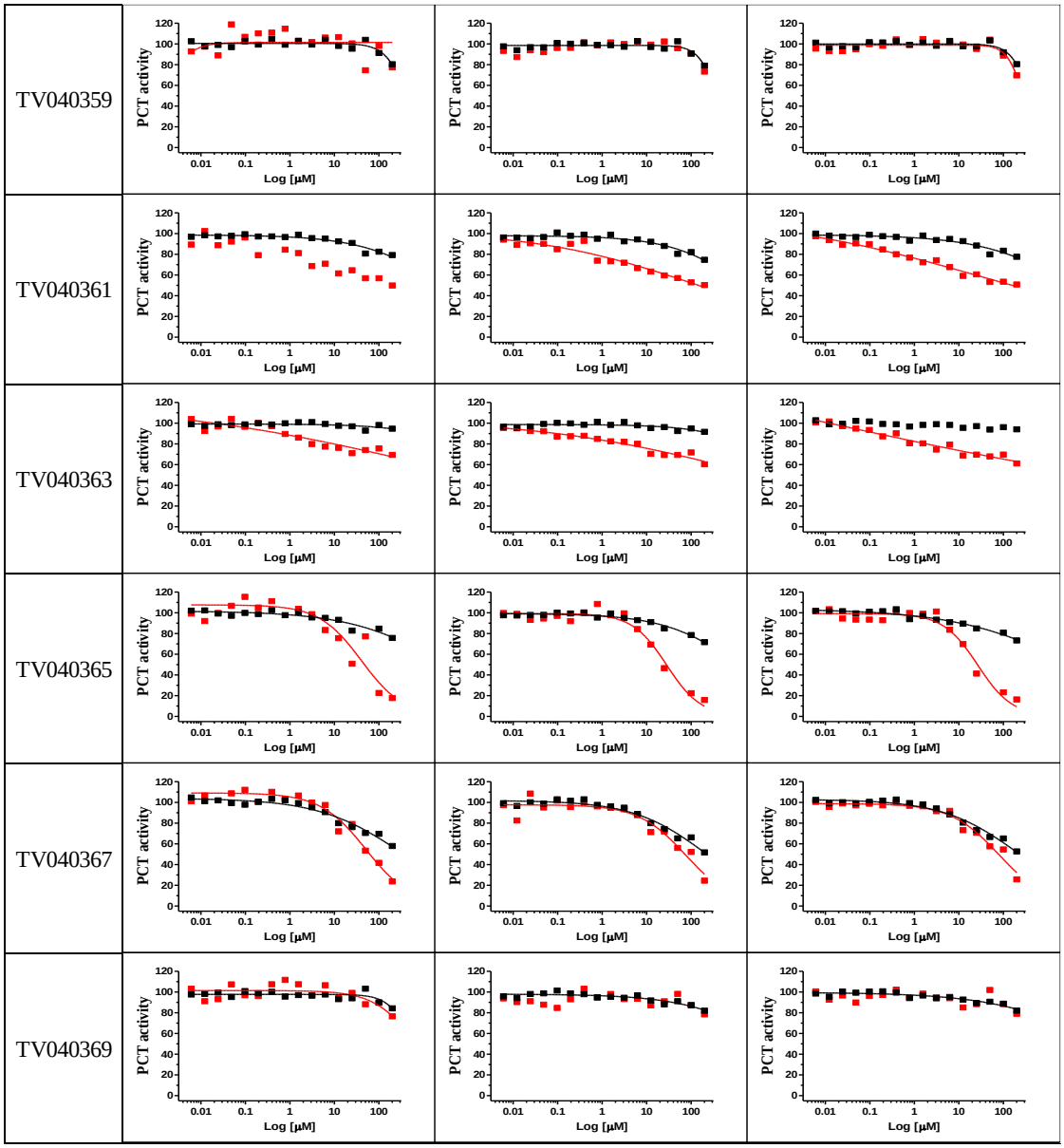

Fig. 3.14. Triplicate IC_{50} curves from dose-response testing of hits from Broad Institute screening in binding assay and counterscreen. Red curves represent dose-reponse binding assay; black curves represent counterscreen.

3.8 Hit Optimization

3.8.1 Optimization of Anabasine

3.8.1.1 Anabasine Ki determination

Previous studies showed that a 12-amino-acid sequence in AF4 that binds to the C-terminus of AF9 potently inhibited binding of AF9 to AF4 with a single-digit nanomolar IC_{50}. Therefore, determination of the Ki of the AF4 12-mer was used to validate the assay method and as a benchmark against which to compare the potency of anabasine and other test compounds. Using a global fit model in GraphPad Prism, the data were fit to the three possible modes of enzyme inhibition: competitive, non-competitive, and uncompetitive. In each case the best fit was to competitive inhibition, giving Ki values for anabasine and AF4 12-mer of 24.3 µM and 14.9 nM, respectively. The 1,630-fold difference between the anabasine Ki and that of the AF4 12-mer indicates weak binding between anabasine and AF9 protein. Nevertheless, the competitive nature of the inhibition suggests that the anabasine directly competes with peptide binding to AF9.

A

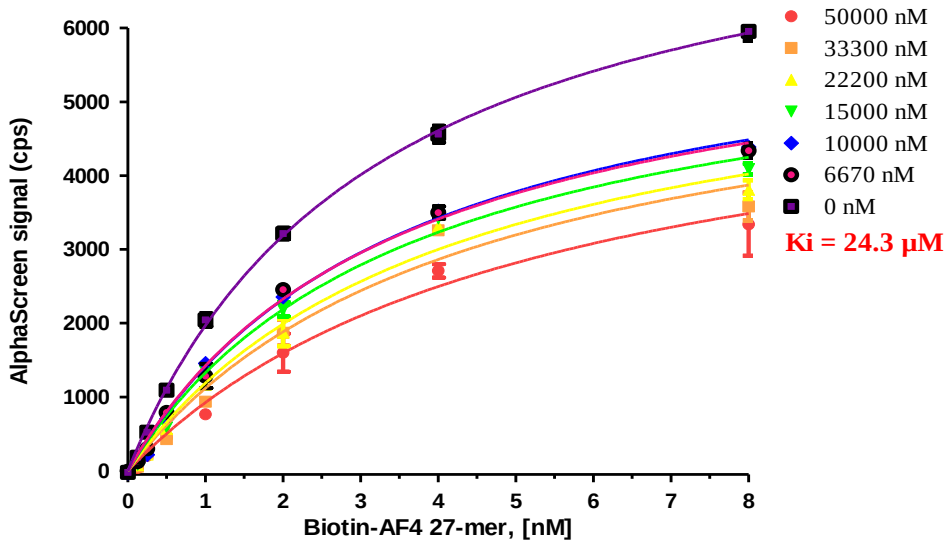

B

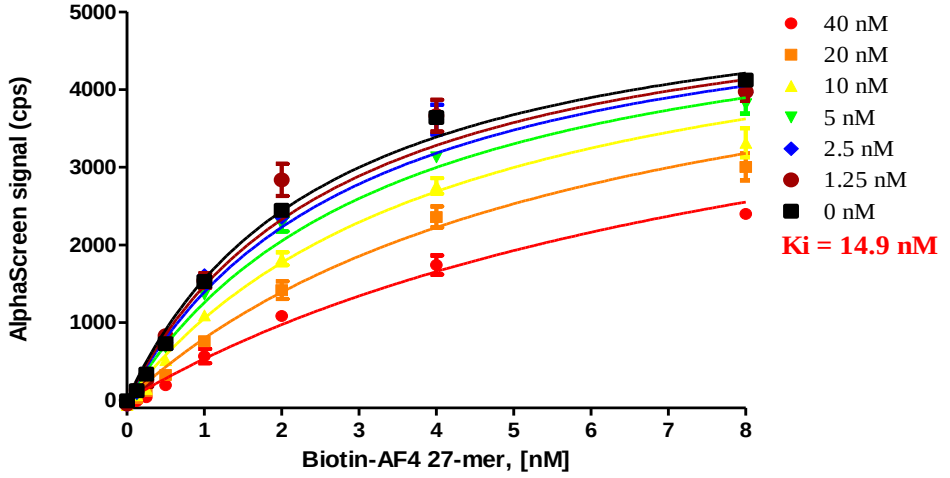

Fig. 3.15. Ki determination of anabasine and AF4 12-mer. (A) Different colors represent different anabasine concentrations. (B) Different colors represent different AF4 12-mer concentrations.

3.8.1.2 Testing of Anabasine Enantiomers and Analogs

Anabasine (TimTec compound ST048429) contains a chiral center in the piperidine ring (Fig. 3.12), so it exists in two enantiomeric forms. The original screening sample is a racemic mixture of the two enantiomers, so Wei Bao in the lab

of Professor John Koh (Dept. of Chemistry and Biochemistry, University of Delaware) synthesized and purified each enantiomer separately so that we could test whether only one enantiomer was responsible for inhibition of AF4-AF9 binding. As protein binding sites are themselves chiral, often only one out of a pair of enantiomers of a small molecule will bind to a target protein. The results in *Table 3.5* showed that the *S*-enantiomer is almost 4-fold more potent than the *R*-enantiomer. Although this is relatively modest difference, it is consistent with selective binding to AF9. The results of testing analogs of anabasine were less encouraging. Minimal activity and poor selectivity was observed among purchased compounds (compound IDs beginning with "Z") or analogs synthesized in the Koh lab (compound IDs beginning with "W"), and none matched or improved on the potency of anabasine itself. Calculated IC_{50} values, dose-response curves, and structures are shown in *Table 3.6*, and *Fig. 3.16*, and *Fig. 3.17*, respectively.

Table 3.5. Inhibition testing of anabasine enantiomer

Anabasine enantiomer	AF4-AF9 binding			Biotin-FLAG counterscreen		Selectivity (Counter IC_{50}/Binding IC_{50})	Triplicate dose-response & counterscreen
	IC_{50} (μM)	Mean IC_{50}	IC_{50} SD	IC_{50} (μM)	Mean IC_{50}		
R form	220.5			>200			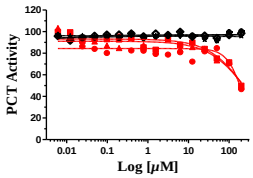
R form	265.8	255.9	31.6	>200	>200	>1	
R form	281.3			>200			
S form	71.0			>200			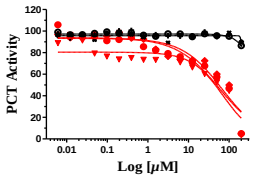
S form	66.3	64.9	7.0	>200	>200	>3	
S form	57.3			>200			
Racemate	97.4		9.4	>200			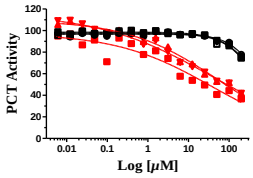
Racemate	109.7	107.7		>200	>200	>2	
Racemate	115.9			>200			

Red curves represent dose-response testing in the binding assay; black curves represent counterscreen.

Table 3.6. Inhibition testing of anabasine analogs

Compound ID	AF4-AF9 binding			Biotin-FLAG counterscreen			Selectivity (Counter IC_{50}/Binding IC_{50})
	IC_{50} (µM)	Mean IC_{50}	IC_{50} SD	IC_{50} (µM)	Mean IC_{50}	IC_{50} SD	
W1573	69.6			264.4			
W1573	81.9	74.1	6.8	308.6	288.5	22.4	3.9
W1573	70.7			292.6			
W1574	156.1		30.1	311.5			
W1574	153.0	137.2		723.1	501.9	207.5	3.7
W1574	102.4			471.0			
SKT678940	5.2			>200			
SKT678940	88.1	60.3		>200	>200		>3
SKT678940	87.5			>200			
W1571	64.6			105.6			
W1571	38.6	48.7	14.0	103.8	105.2	1.2	2.2
W1571	42.8			106.2			
W1552	332.7						
W1552		320.9	16.8	419.9	434.6	20.8	1.4
W1552	309.0			449.3			
Z31662681	>200			>200			
Z31662681	>200	>200		>200	>200		Inactive
Z31662681	>200			>200			
Z31976552	>200			>200			
Z31976552	>200	>200		>200	>200		Inactive
Z31976552	>200			>200			
Z33442216	>200			>200			
Z33442216	>200	>200		>200	>200		Inactive
Z33442216	>200			>200			
Z33442392	>200			>200			
Z33442392	>200	>200		>200	>200		Inactive
Z33442392	>200			>200			
W1271	>200			>200			
W1271	>200	>200		>200	>200		Inactive
W1271	>200			>200			

W1272	>200		>200		
W1272	>200	>200	>200	>200	Inactive
W1272	>200		>200		
W1273	>200		>200		
W1273	>200	>200	>200	>200	Inactive
W1273	>200		>200		
W1275	>200		>200		
W1275	>200	>200	>200	>200	Inactive
W1275	>200		>200		
W1501	>200		>200		
W1501	>200	>200	>200	>200	Inactive
W1501	>200		>200		
W1553	>200		>200		
W1553	>200	>200	>200	>200	Inactive
W1553	>200		>200		
W1554	>200		>200		
W1554	>200	>200	>200	>200	Inactive
W1554	>200		>200		
W1555	>200		>200		
W1555	>200	>200	>200	>200	Inactive
W1555	>200		>200		
W1556	>200		>200		
W1556	>200	>200	>200	>200	Inactive
W1556	>200		>200		
W1575	>200		>200		
W1575	>200	>200	>200	>200	Inactive
W1575	>200		>200		
W165	>200		>200		
W165	>200	>200	>200	>200	Inactive
W165	>200		>200		

Compound ID	Plate 1	Plate 2	Plate 3
Z31662681	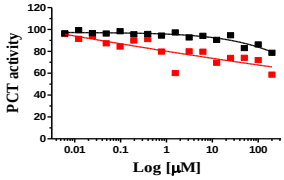	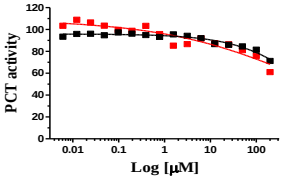	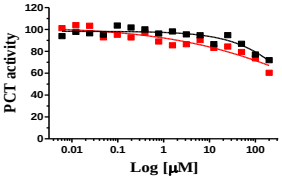
Z31976552	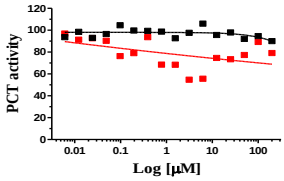	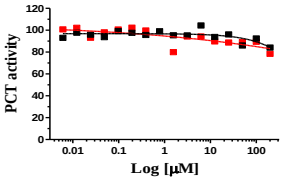	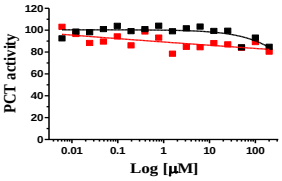
Z33442216	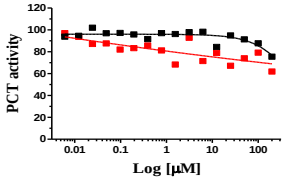	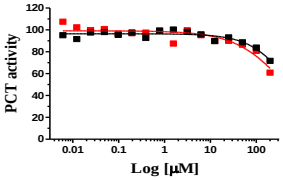	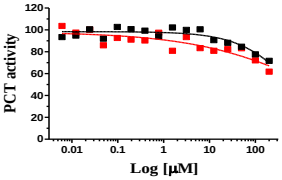
Z33442392	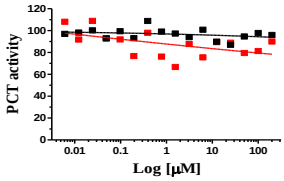	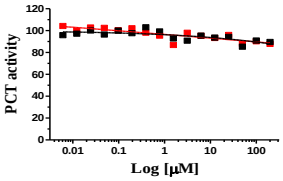	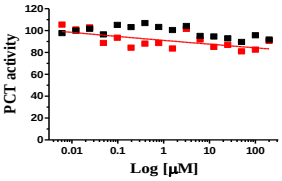
SKT678940	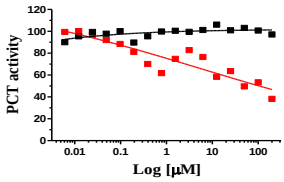	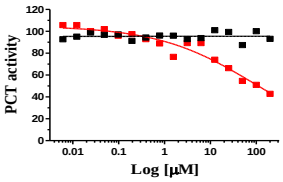	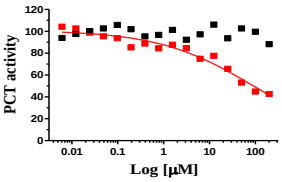

W1271	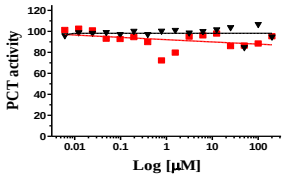	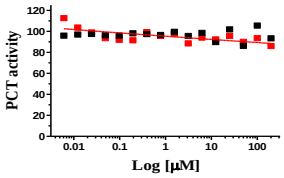	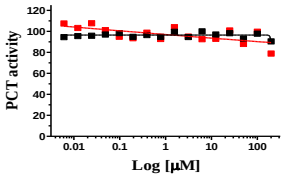
W1272	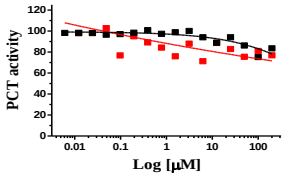	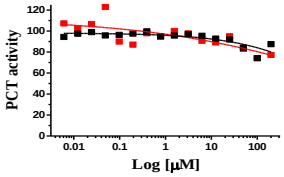	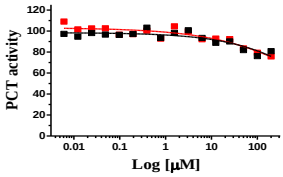
W1273	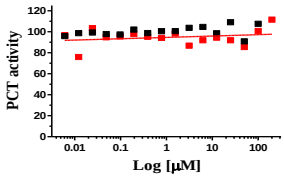	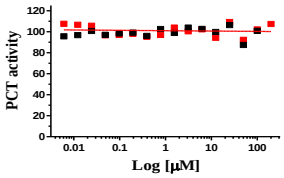	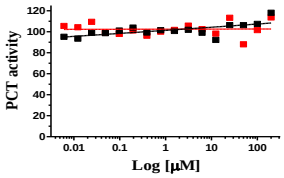
W1275	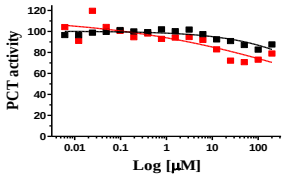	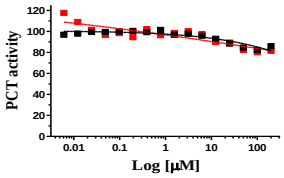	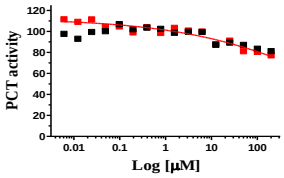
W1501	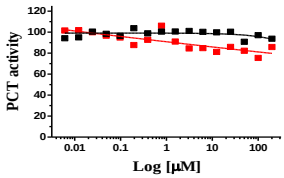	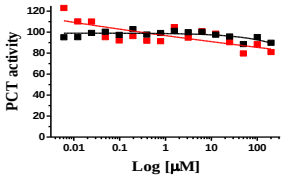	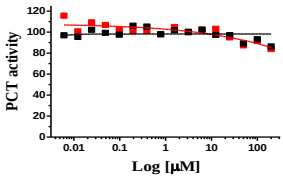

W1552	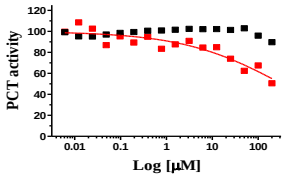	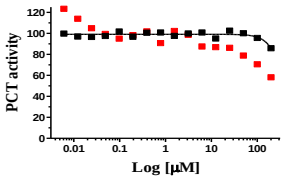	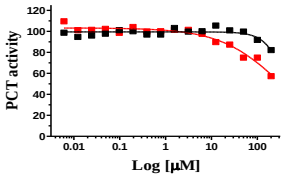
W1553	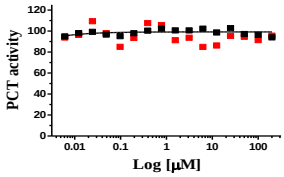	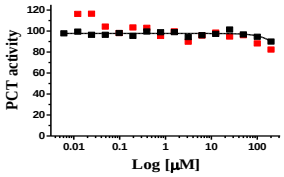	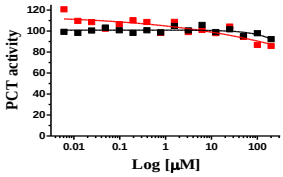
W1554	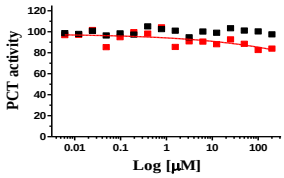	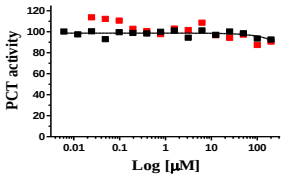	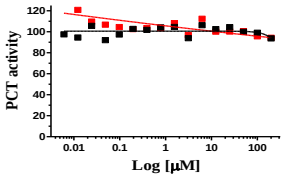
W1555	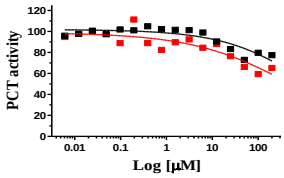	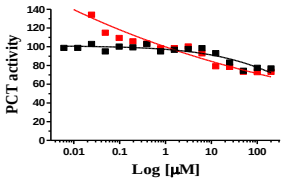	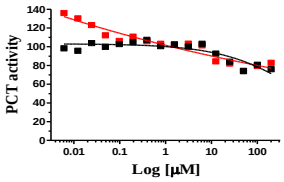
W1556	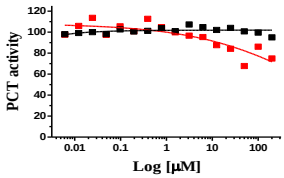	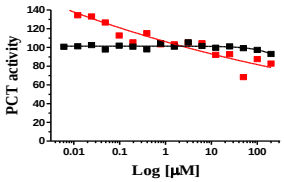	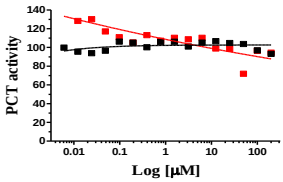

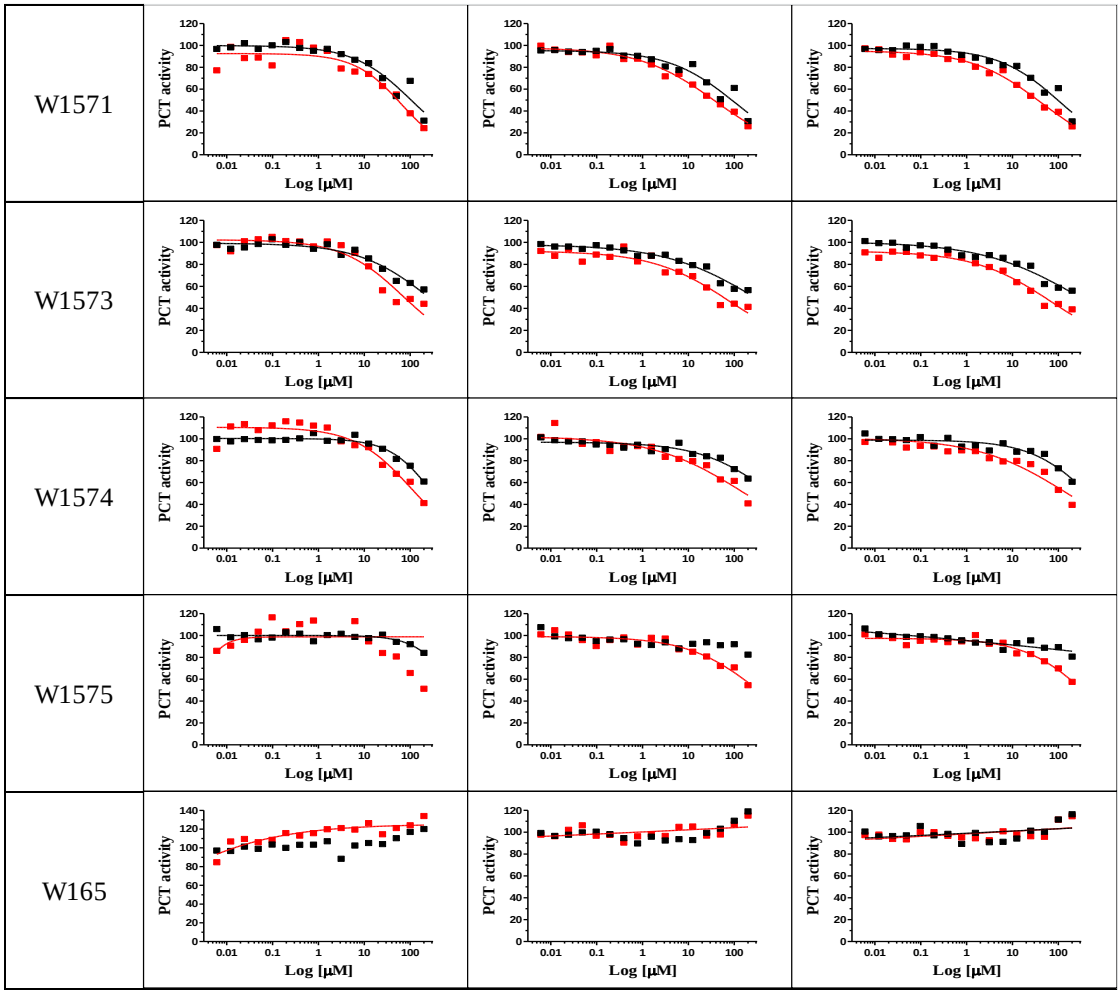

Fig. 3.16. Triplicate IC_{50} curves from dose-response testing of anabasine analogs in the binding assay and counterscreen. Red curves represent binding assay; black curves represent counterscreen.

Anabasine from different sources was also tested in dose-response. However, none of the solid samples matched the potency of the solution of anabasine in DMSO tested in the original screen (Figure 3.18). Also, the original screening sample gave a sigmoidal IC_{50} curve (shown in the upper left panel of *Figure 3.18*), whereas the curves obtained from the solid samples of anabasine were less steep and did not reach full inhibition of AF4-AF9 binding even at the highest concentrations tested. Often, less than "ideal" dose-response profiles such as these suggest that the activity does not

arise from a single well-defined entity. Similarly, low potency was also observed upon testing the enantiomers of anabasine (Table 3.6). It seems that progressively lower potency was observed as the anabasine was more highly purified: purity of anabasine solution in original screen < purity of commercial available solids < chemically synthesized solids. These results suggest that the high potency observed in the original screen might be due to inhibition caused by an impurity in the DMSO solution of anabasine.

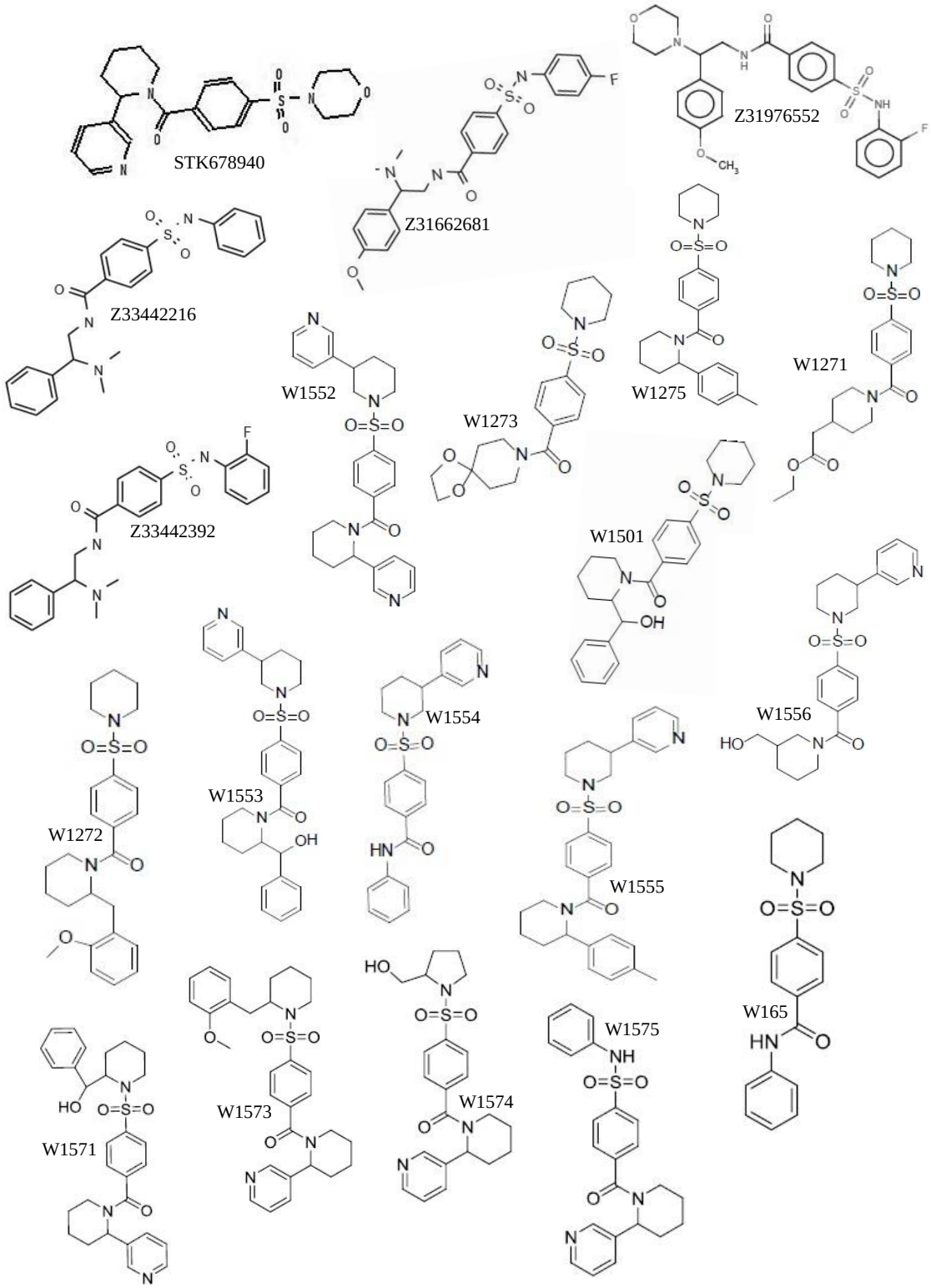

Fig. 3.17. Structures of anabasine analogs

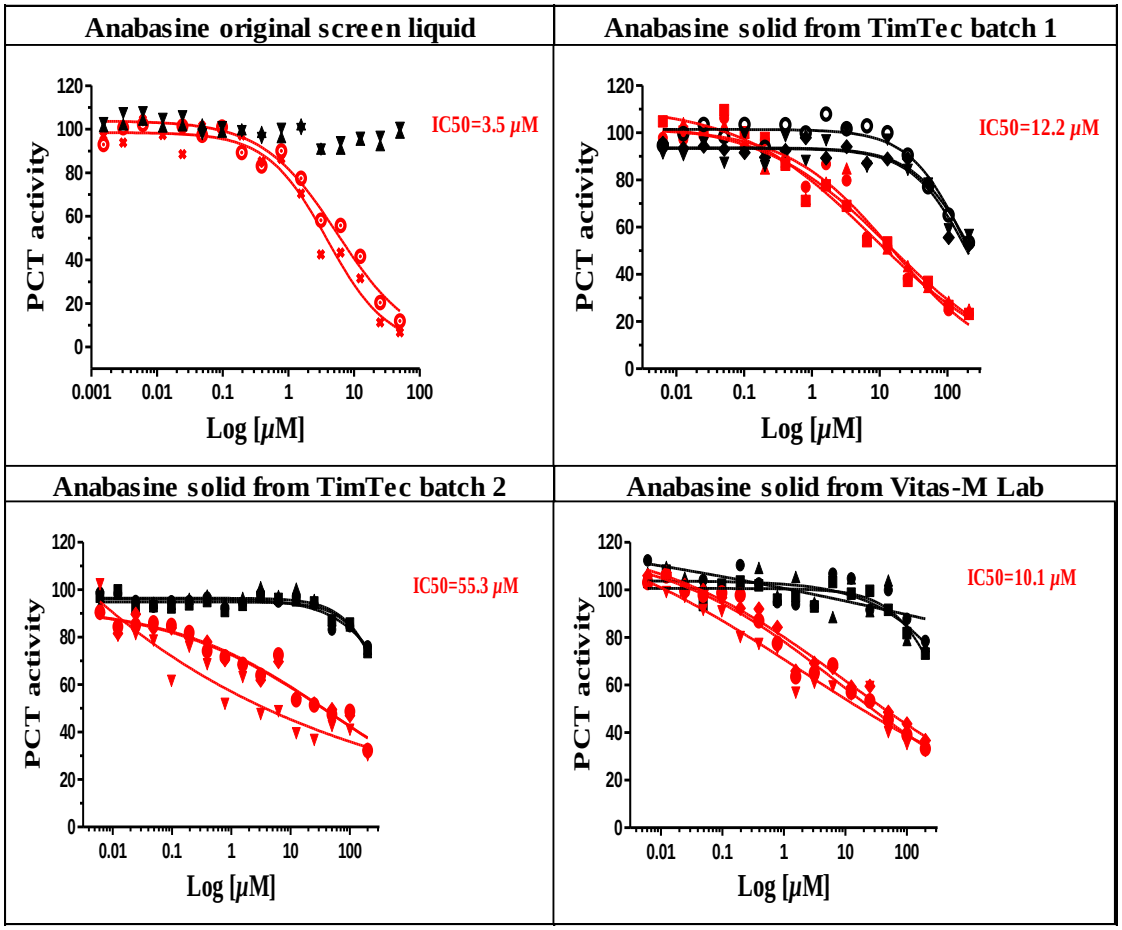

Fig. 3.18. Testing of anabasine from different sources. Red curves represent binding assay with Biotin-AF4 and AF9-FLAG. Black curves represent counterscreen with Biotin-FLAG.

3.8.2 Optimization of Compound from Broad Institute Screening

After unsuccessful optimization of anabasine we moved our focus to compound TV040365 discovered in the Broad Institute screen of the NIH compound library. In contrast to anabasine, TV040365 exhibited a good fit to a sigmoidal dose-response curve, showed complete inhibition at the highest concentrations tested, a gave good selectivity between the binding assay and the counterscreen (Figure 3.19).

Overall, these results indicate that TV040365 is a promising compound to be further optimized.

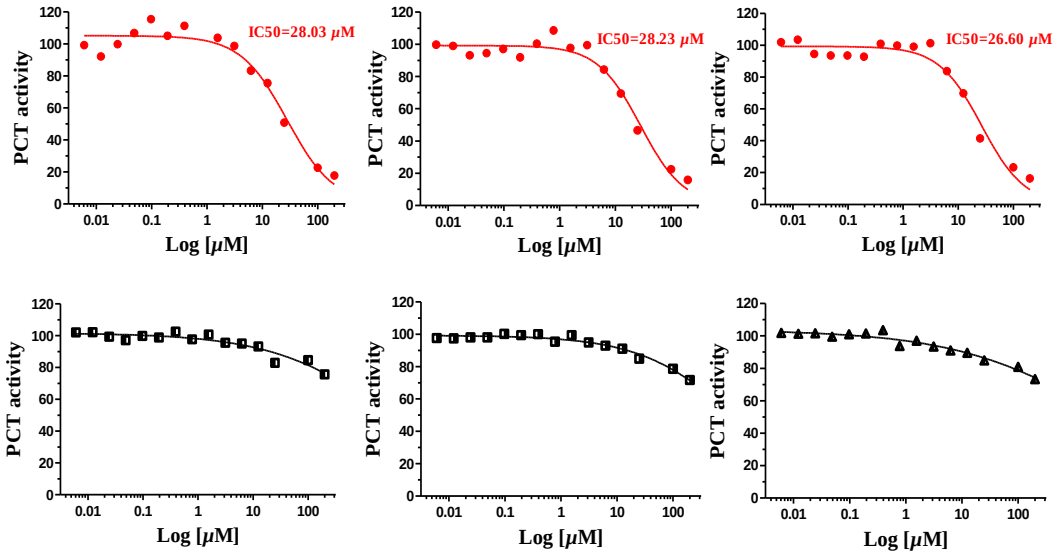

Fig. 3.19. Inhibition testing of Broad Institute compound TV040365. Red curves represent dose-response binding assay with Biotin-AF4 and AF9-FLAG. Black curves represent counterscreen with Biotin-FLAG.

3.8.2.1 TV040365 Ki determination

TV040365 gave a Ki >3-fold less than the Ki of anabasine (Fig. 3.20 A), indicating stronger binding of TV040365 to AF9 protein. Also, the inhibition fit best to a competitive pattern, suggesting that the TV040365 directly competes with peptide binding to AF9.

A

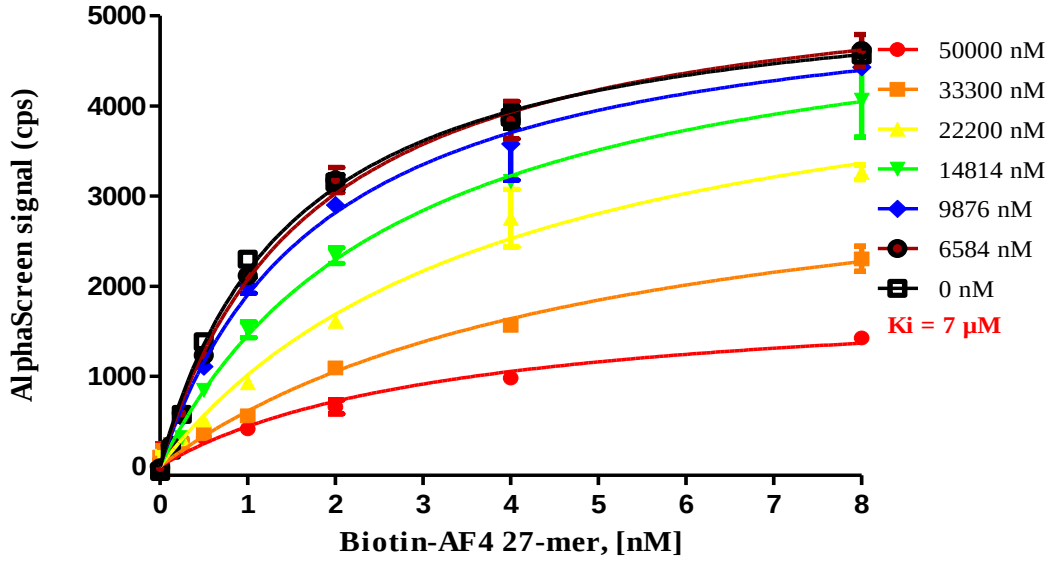

B

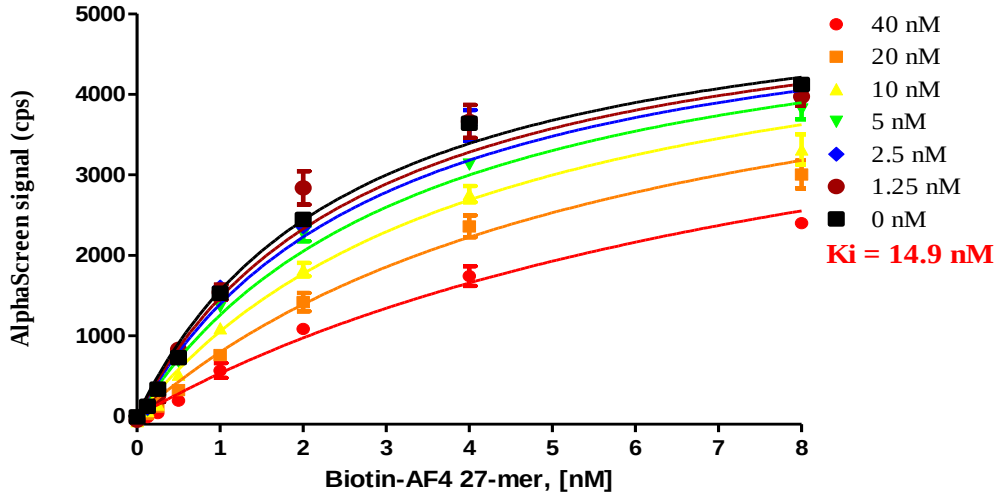

Fig. 3.20. Ki determination of TV040365 and AF4 12-mer. (A) Different colors represent different TV040365 concentrations. (B) Different colors represent different AF4 12-mer concentrations.

3.8.2.2 Testing of TV040365 Analogs

Six TV040365 analogs synthesized by Wei Bao were tested in dose-response in the AF4-AF9 binding assay and biotin-FLAG counterscreen (see Fig. 3.22 for structures). W188 had the best combination of potency and selectivity. Its IC_{50} was approximately equal to that of TV040365 (Fig. 3.19), and it showed selectivity of at least 6-fold vs. the counterscreen (Table 3.7, Fig. 3.21). Although none of these analogs showed better potency than TV040365, it is nevertheless encouraging that 4 out of 6 analogs showed potency within 4-fold of that of TV040365 without affecting the counterscreen. These results will provide the basis for synthesis and testing of additional analogs with the goal of identifying inhibitors with greater potency than TV040365.

Table 3.7. Inhibition testing of TV040365 analogs

Compound ID	AF4-AF9 binding			Biotin-FLAG counterscreen			Selectivity (Counter IC_{50}/Binding IC_{50})
	IC_{50} (μM)	Mean IC_{50}	IC_{50} SD	IC_{50} (μM)	Mean IC_{50}	IC_{50} SD	
W188	35.3			>200			
W188	34.1	36.5	3.1	>200	>200		>6
W188	40.0			>200			
DR17	59.4			>200			
DR17	49.4	54.0	5.0	>200	>200		>4
DR17	53.2			>200			
W194	57.4			>200			
W194	63.2	61.4	3.5	>200	>200		>3
W194	63.7			>200			
W187	142.8			>200			
W187	126.6	112.1	40.0	>200	>200		>2
W187	66.8			>200			
W193	10.8			26.3			
W193	8.6	10.2	1.4	31.2	27.8	2.9	2.73
W193	11.2			26.0			
DR25	>200			>200			
DR25	>200	>200		>200	>200		Inactive
DR25	>200			>200			

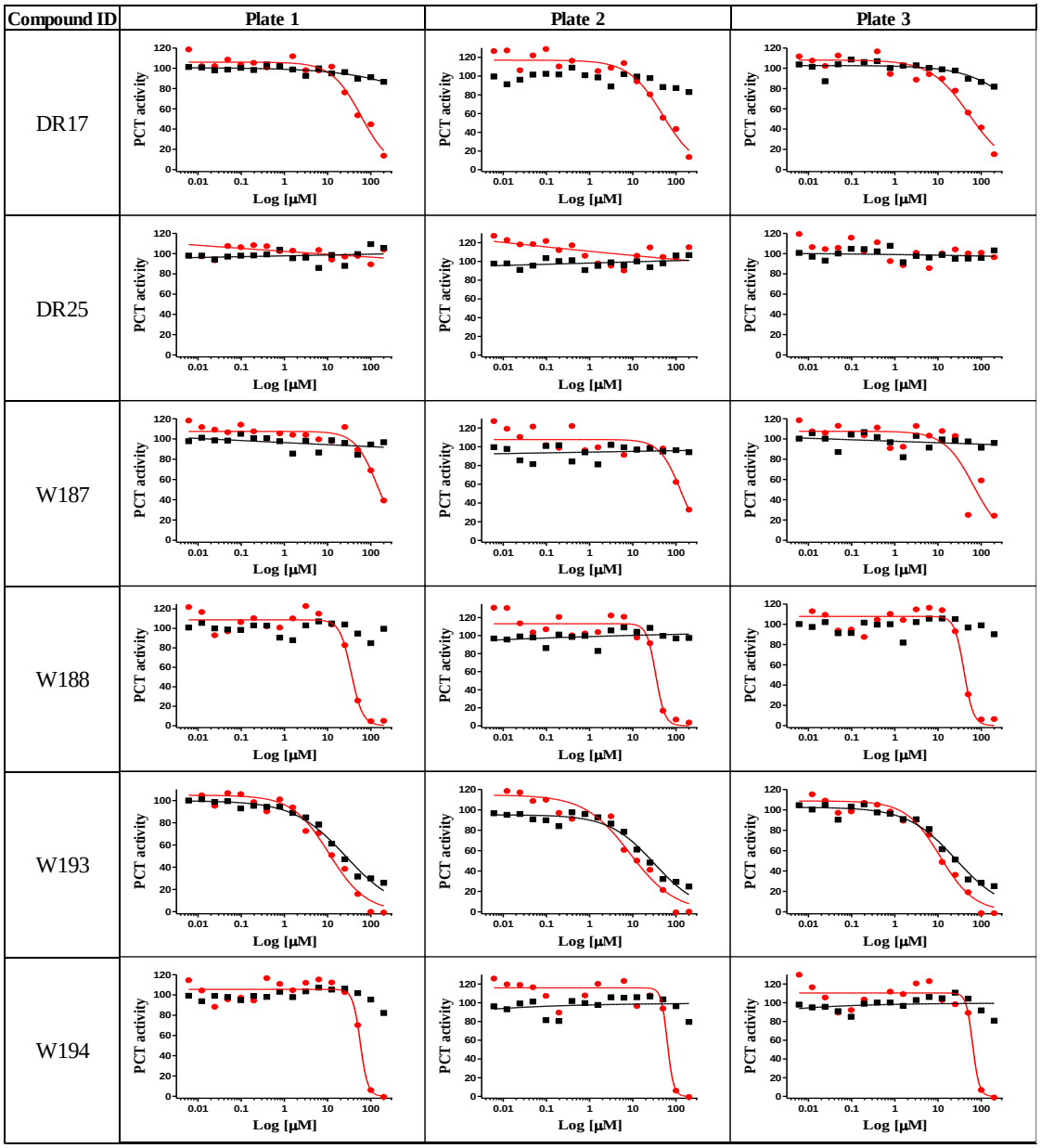

Fig. 3.21. Triplicate IC_{50} curves from dose-response testing of Broad Institute compound TV040365 screening in binding assay and counterscreen. Red curves represent dose-response binding assay; black curves represent counterscreen.

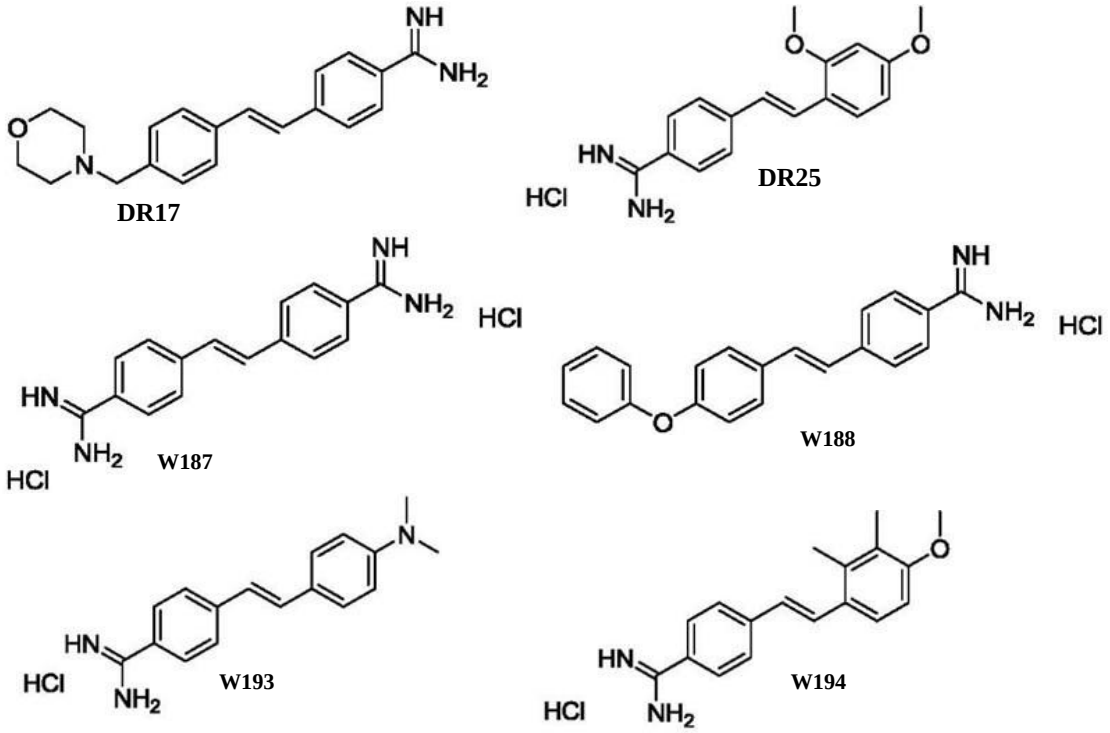

Fig. 3.22. Structures of TV040365 analogs.

Chapter 4

DISCUSSION

To discover inhibitors of the interaction of MLL-AF4 and AF9 in MLL-R leukemia, an AlphaScreen assay comprising AF9 protein and a peptide derived from AF4 was used to screen 96,000 compounds at Nemours, and 350,000 compounds at the Broad Institute in Cambridge, MA. To minimize the reagent costs and time of screening at Nemours, an orthogonal pooling method was validated and used to screen libraries as mixtures of 10 compounds per well.

AlphaScreen is a versatile and sensitive technology for the detection of the protein–protein and protein–peptide interactions. However, even after optimization, the assay is prone to compound effects unrelated to the targeted protein–peptide binding interaction. The susceptibility of AlphaScreen to artifacts interfering with bead capture or energy transfer was evident from the high primary hit rate obtained in the LCGC and Broad Institute screens. However, with counterscreen using biotin-FLAG, a reagent that contains both bead capture tags in a single molecule, it is possible to readily identify these artifacts and exclude them from further study.

After exclusion of assay artifacts, and confirmation of the activity of screening hits by testing of freshly made solutions of test compounds from solids, compounds that showed promising activity and had structures amenable to chemical modification were selected for further study. One compound, anabasine (Fig. 3.11), was identified following pilot screening performed earlier by Kathy Drake and Venita Watson; a second compound showing good activity, TV040365 (Fig. 3.13), was discovered in

the NIH library at the Broad Institute. Analogs of both compounds were synthesized in the lab of Dr. John Koh at the University of Delaware and tested for activity by me here at Nemours.

In addition to testing of analogs, selectivity of the inhibitors for the AF9 protein was evaluated by determining the inhibition constant Ki and the mode of inhibition. In the case of both anabasine and TV040365, inhibition appeared to be competitive with AF4-derived peptide, consistent with compound binding directly to AF9. In the case of anabasine, separate testing of its two enantiomers was used as a further measure of selectivity. A modest difference in potency between the two enantiomers provided some evidence of compound binding to the chiral protein surface.

After consideration of the test data obtained for anabasine and analogs, it was decided to suspend work on this compound. The activity of test samples appeared to decrease as the extent of purity increased, suggesting that the original screening sample may have contained an active impurity that would be very difficult to identify. Also, none of the analogs were active, so there is no clear path towards improved potency. In contrast, the data obtained so far on TV040365 looks promising. A solid sample of the original hit consistently shows reasonable activity, and several analogs were also found to be active. Further work will continue to explore the structure-activity relationships to find compounds of sufficient potency to test in leukemia cells.

Chapter 5

FUTURE DIRECTION OF THE PROJECT

For hits to be useful as chemical probes to explore the biology of MLL-R leukemia and to be advanced as potential therapeutic leads, it is essential that they selectively disrupt MLL-AF4 binding to AF9 in MLL-R leukemia cells. Hemenway and coworkers have shown that cell-penetrating peptides derived from AF4 disrupt the AF4-AF9 interaction and cause cell death preferentially in MLL-R leukemia cell lines [15, 16]. Thus, optimization of compound TV040365 and analogs will continue, and if necessary more compound libraries will be screened to obtain inhibitors that bind to AF9 that will be studied for their effect on cell viability in leukemic cell lines. Based on the peptide work in the Hemenway group, it is our expectation that AF9-binding compounds will selectively kill leukemic cells that harbor the MLL-AF4 fusion over those that do not bear the fusion. Such compounds should hold significant promise as potential therapeutic leads, and will be further advanced to animal testing in a mouse model of engrafted leukemia [25].

Successful testing of AF9 inhibitors against leukemia *in vivo* will provide compounds for pre-clinical optimization and potential candidates for the treatment of infants and children with leukemia harboring MLL fusions. Ultimately, compounds identified as potent and selective hits through these efforts may serve as leads in the development of targeted therapies for MLL-R leukemias.

REFERENCES

1. Muntean, A.G. and J.L. Hess, *The pathogenesis of mixed-lineage leukemia.* Annu Rev Pathol, 2012. **7**: p. 283-301.

2. Slany, R.K., *The molecular biology of mixed lineage leukemia.* Haematologica, 2009. **94**(7): p. 984-93.

3. Robinson, B.W., Devidas, M., Carroll, A.J., Harvey, R.C., Heerema, N.A., Willman,C.L.,etal., *Specific MLL partner genes in infant acute lymphoblastic leukemia (ALL) associated with outcome are linked to age and white blood cell count (WBC) at diagnosis are port on the Children's Oncology Group (COG) P9407 trial.* in American Society of Hematology Annual Meeting and Exposition, 2009.

4. Hess, J.L., et al., *Defects in yolk sac hematopoiesis in Mll-null embryos.* Blood, 1997. **90**(5): p. 1799-806.

5. Milne, T.A., et al., *MLL targets SET domain methyltransferase activity to Hox gene promoters.* Mol Cell, 2002. **10**(5): p. 1107-17.

6. Yu, B.D., et al., *MLL, a mammalian trithorax-group gene, functions as a transcriptional maintenance factor in morphogenesis.* Proc Natl Acad Sci U S A, 1998. **95**(18): p. 10632-6.

7. Yu, B.D., et al., *Altered Hox expression and segmental identity in Mll-mutant mice.* Nature, 1995. **378**(6556): p. 505-8.

8. Armstrong, S.A., T.R. Golub, and S.J. Korsmeyer, *MLL-rearranged leukemias: insights from gene expression profiling.* Semin Hematol, 2003. **40**(4): p. 268-73.

9. Armstrong, S.A., et al., *MLL translocations specify a distinct gene expression profile that distinguishes a unique leukemia.* Nat Genet, 2002. **30**(1): p. 41-7.

10. Faber, J., et al., *HOXA9 is required for survival in human MLL-rearranged acute leukemias.* Blood, 2009. **113**(11): p. 2375-85.

11. Monroe, S.C., et al., *MLL-AF9 and MLL-ENL alter the dynamic association of transcriptional regulators with genes critical for leukemia.* Exp Hematol, 2011. **39**(1): p. 77-86 e1-5.

12. Bitoun, E., P.L. Oliver, and K.E. Davies, *The mixed-lineage leukemia fusion partner AF4 stimulates RNA polymerase II transcriptional elongation and mediates coordinated chromatin remodeling.* Hum Mol Genet, 2007. **16**(1): p. 92-106.

13. Meyer, C., et al., *The MLL recombinome of acute leukemias.* Leukemia, 2006. **20**(5): p. 777-84.

14. Huret, J.L., P. Dessen, and A. Bernheim, *An atlas of chromosomes in hematological malignancies. Example: 11q23 and MLL partners.* Leukemia, 2001. **15**(6): p. 987-9.

15. Palermo, C.M., et al., *The AF4-mimetic peptide, PFWT, induces necrotic cell death in MV4-11 leukemia cells.* Leuk Res, 2008. **32**(4): p. 633-42.

16. Srinivasan, R.S., et al., *The synthetic peptide PFWT disrupts AF4-AF9 protein complexes and induces apoptosis in t(4;11) leukemia cells.* Leukemia, 2004. **18**(8): p. 1364-72.

17. Erfurth, F., et al., *MLL fusion partners AF4 and AF9 interact at subnuclear foci.* Leukemia, 2004. **18**(1): p. 92-102.

18. Bennett, C.A., et al., *Molecular targeting of MLL-rearranged leukemia cell lines with the synthetic peptide PFWT synergistically enhances the cytotoxic effect of established chemotherapeutic agents.* Leuk Res, 2009. **33**(7): p. 937-47.

19. Kazmierski, W.M., T.P. Kenakin, and K.S. Gudmundsson, *Peptide, peptidomimetic and small-molecule drug discovery targeting HIV-1 host-cell attachment and entry through gp120, gp41, CCR5 and CXCR4.* Chem Biol Drug Des, 2006. **67**(1): p. 13-26.

20. Watson, V.G., et al., *Development of a high-throughput screening-compatible assay for the discovery of inhibitors of the AF4-AF9 interaction using AlphaScreen technology.* Assay Drug Dev Technol, 2013. **11**(4): p. 253-68.

21. MicroSource. Available from: http://www.msdiscovery.com/spectrum.html.

22. TimTec. Available from: http://www.timtec.net/Natural-Products.html.

23. Motlekar, N., S.L. Diamond, and A.D. Napper, *Evaluation of an orthogonal pooling strategy for rapid high-throughput screening of proteases.* Assay Drug Dev Technol, 2008. **6**(3): p. 395-405.

24. Zhang, J.H., T.D. Chung, and K.R. Oldenburg, *A Simple Statistical Parameter for Use in Evaluation and Validation of High Throughput Screening Assays.* J Biomol Screen, 1999. **4**(2): p. 67-73.

25. Lee, E.M., P.S. Bachmann, and R.B. Lock, *Xenograft models for the preclinical evaluation of new therapies in acute leukemia.* Leuk Lymphoma, 2007. **48**(4): p. 659-68.